



**KTH Engineering Sciences**

# **Maximization of the Wehrl Entropy in Finite Dimensions**

ANNA BÆCKLUND

Master of Science Thesis  
Stockholm, Sweden 2013  
Supervisor: Ingemar Bengtsson

TRITA-FYS 2013:07



### Abstract

The Wehrl entropy is the entropy of the probability distribution in phase space corresponding to the Husimi function in terms of coherent states. We explain the significance of the Wehrl entropy in quantum information theory, and present the theory behind the Lieb conjecture, which states that, in finite dimensions, the minimum Wehrl entropy occurs for Bloch coherent states. This was proven by Lieb and Solovej in 2012.

We present the theory behind coherent states, with a particular emphasis on Bloch coherent states, and give a geometrical representation of quantum states as points on a sphere. Using this representation, we identify spherical arrangements of 2–9 points that maximize the Wehrl entropy locally. We conjecture that these maxima are in fact global. Furthermore, we investigate how the maximally entangled symmetric states are related to the states corresponding to maximal Wehrl entropy.

## Sammanfattning

Wehrlentropin är den entropi som ges av den sannolikhetsfördelning i fasrummet som motsvarar Husimifunktionen i termer av koherenta tillstånd. Vi förklarar Wehrlentropins betydelse inom ämnet kvantinformation samt teorin bakom Liebs förmodan. Enligt denna antar Wehrlentropin för ändliga dimensioner sitt minsta värde för Bloch-koherenta tillstånd. Liebs förmodan bevisades av Lieb och Solovej 2012.

Vi presenterar teorin bakom koherenta tillstånd, med särskild betoning på Bloch-koherenta tillstånd, och representerar kvantmekaniska tillstånd geometriskt som punkter på en sfär. Med hjälp av denna representation identifierar vi sfäriska arrangemang av 2-9 punkter som lokalt maximerar Wehrlentropin. Vi förmodar att dessa maxima även är globala. Vidare undersöker vi sambandet mellan de maximalt snärjda symmetriska tillstånden och de tillstånd som motsvarar maximal Wehrlentropi.

# Contents

<b>Contents</b>	<b>v</b>
<b>Preface</b>	<b>vii</b>
<b>1 Introduction</b>	<b>1</b>
<b>2 Background Material</b>	<b>3</b>
2.1 Basic Concepts . . . . .	3
2.2 The Stellar Representation . . . . .	7
<b>3 Coherent States</b>	<b>11</b>
3.1 Canonical Coherent States . . . . .	11
3.2 Bloch Coherent States . . . . .	14
<b>4 Wehrl Entropy</b>	<b>19</b>
4.1 Husimi Function . . . . .	19
4.2 Wehrl Entropy . . . . .	21
4.3 Problem Description . . . . .	26
4.4 Optimal Arrangements . . . . .	29
4.5 Results . . . . .	30
4.6 Comment on the Proof of the Lieb Conjecture . . . . .	40
<b>5 Geometric Entanglement of Symmetric States</b>	<b>47</b>
5.1 Geometric Measure of Entanglement . . . . .	48
5.2 Highest Geometric Entanglement Configurations . . . . .	50
<b>6 Summary and Conclusions</b>	<b>55</b>
<b>Bibliography</b>	<b>57</b>
<b>A SU(2)</b>	<b>61</b>



# Preface

This thesis is the result of my Master of Science degree project, which was carried out at the Department of Theoretical Physics at the Royal Institute of Technology (KTH), and the Department of Quantum Information and Quantum Optics at Stockholm University during the autumn of 2012 and winter of 2013. I would like to thank my supervisor Ingemar Bengtsson for valuable guidance. I would also like to thank my friends for their help, as well as my family for all their support.





# Chapter 1

## Introduction

In the past 50 years the entropy concept has become increasingly important in information theory, which is one of the foundations of quantum information. One important feature in quantum information is entanglement, which refers to the strong quantum correlations that two or more quantum particles can possess. Another feature is uncertainty, which lies at the heart of quantum theory. The uncertainty in classical information theory is present due to a lack of total information. Quantum uncertainty, on the other hand, does not arise due to a lack of information, but is rather a fundamental uncertainty inherent in nature itself, arising from the Heisenberg uncertainty principle.

In this work we focus on entropy as a measure the coherence of a system, that is, a measure of how classical a system is. One might expect a measure of the entropy of a quantum system to be very different from the classical measure of entropy, because a quantum system possesses not only classical uncertainty but also quantum uncertainty. However, the density operator captures both types of uncertainty, which allows probabilities for the outcome of any measurement on the system to be determined. Thus a quantum measure of uncertainty should be a direct function of the density operator, just as the classical measure of uncertainty is a direct function of a probability density function [30].

There are several quantum information measures, such as the von Neumann entropy which determines how much quantum information there is in a quantum system. However, the von Neumann entropy becomes zero for all pure states, and can therefore not be used in discriminating between them. Instead the Wehrl entropy [19] is chosen as a classicality measure. Wehrl used coherent states to define the Wehrl entropy as a new concept of the classical entropy of a quantum state. These are, in a sense, the most classical quantum states. In a geometric representation of a state of spin  $j$  as  $2j$  points on a sphere, a coherent state corresponds to coinciding points.

The Wehrl entropy is minimized by the coherent states [15]. As the system becomes more quantum, meaning that the points on the Bloch sphere spread further

apart, the Wehrl entropy increases. The purpose of this investigation is to maximize the Wehrl entropy. We define the most non-coherent states, which are the 'most quantum' states, as the states for which maximum Wehrl entropy occurs. These most non-coherent states correspond to spherical arrangements of points that are as far away from each other as possible. Thus the resulting problem consists of distributing the points so that the Wehrl entropy is maximized, at least locally. In solving this problem we utilize the fact that if the eigenvalues of the Hessian at a critical arrangement are all negative, then that arrangement yields a local maximum.

Before dealing with this problem we will review some basic concepts. We begin our study in Chapter 2 by defining the Bloch sphere and deriving the stellar representation, which is a one-to-one correspondence between pure quantum states and points on a sphere. In Chapter 3 we introduce the coherent states, with an emphasis on the Bloch coherent states, and explain some of their properties.

Moving on to our actual investigations in Chapter 4, we shall begin by describing the Wehrl entropy and the Lieb conjecture. Here the stellar representation is used to represent states by points on a sphere. By means of the Stellar representation we present spherical arrangements of 2-9 points on the unit sphere that maximize the Wehrl entropy. This is the main goal of the thesis. We also compare the spectra for the von Neumann entropy and Wehrl entropy, and show that the most non-coherent states correspond to maxima in both entropies.

In Chapter 5 we explore the maximally entangled symmetric states of 2-9 qubits and their amount of geometric entanglement, and investigate how these states are related to the states corresponding to maximal Wehrl entropy. Chapter 6 consists of a summary and conclusion of this thesis.

## Chapter 2

# Background Material

We begin this chapter by defining and discussing some basic concepts that will be needed in chapters to come. We provide a fairly brief review of a visualization of a state space and present the idea of representing points in the complex projective space  $\mathbb{C}\mathbf{P}^n$  as stars on a sphere. The material covered in this chapter can be found in Refs. [1–5].

### 2.1 Basic Concepts

#### Bloch Sphere Representation

In this section we introduce the Bloch sphere, which is a spherical representation of the physical states described by a two-dimensional Hilbert space, also known as a two-level system or a two-state system. A two-level system can be mapped onto a spin-1/2 system by assigning one state to the eigenstate with eigenvalue  $+1/2$  (spin up) and the orthogonal state to the eigenstate with eigenvalue  $-1/2$  (spin down). An interesting property of a spin-1/2 system is that it can be interpreted as a qubit of spin up in some direction. From this it is clear that the space of all qubits constitute a sphere, i.e. 'the set of all directions'.

A general pure state in a two-level system can be built from a superposition of a spin-up and spin-down state. We present how the set of all normalized pure states in the two-dimensional Hilbert space can be represented by the surface of a sphere, i.e. the Bloch sphere. We then continue by explaining the relation between pure states and points on the Bloch sphere.

Consider the superposition state

$$|\psi\rangle = \psi_1|0\rangle + \psi_2|1\rangle. \quad (2.1)$$

This can be represented by a point on a unit sphere defined by a unit vector  $\mathbf{n}$ , where a spin-up state corresponds to the north pole and a spin-down state corresponds to the south pole. The state is specified by the relative amplitude and phase of its

two components (we ignore the normalization factor and overall phase). These two parameters can be mapped to the spherical coordinates  $\theta$  and  $\phi$ ,

$$\begin{aligned} |\psi\rangle &= \psi_1|0\rangle + \psi_2|1\rangle = \psi_1(|0\rangle + z|1\rangle) \\ &\sim \cos\frac{\theta}{2}|0\rangle + e^{i\phi}\sin\frac{\theta}{2}|1\rangle, \quad 0 \leq \theta < \pi, \quad 0 \leq \phi < 2\pi, \end{aligned} \quad (2.2)$$

which specify the direction of  $\mathbf{n}$ . Thus the superposition state  $|\psi\rangle$  can be interpreted as a spin pointing in the  $(\theta, \phi)$  direction, with its antipodal point representing the opposite state. We note that the complex number  $z = \frac{\psi_2}{\psi_1} = e^{i\phi} \tan\frac{\theta}{2}$  can take any value in the extended complex plane  $\mathbb{C}_\infty = \mathbb{C} \cup \{\infty\}$  and, in particular, for  $\psi_1 = 0$  we have that  $z = \infty$ .

It is natural to interpret (2.1) as the spin state of a spin-1/2 particle like the electron. Then  $|0\rangle$  and  $|1\rangle$  are the spin-up and spin-down states along a particular axis, such as the  $z$ -axis. As a result, the point where  $\mathbf{n}$  meets the sphere could equally well be viewed as an eigenstate with eigenvalue  $+1/2$  for a spin oriented along the spatial direction  $\mathbf{n}$ .

### Stereographic Projection

We now establish a one-to-one correspondence between the Bloch sphere and the extended complex plane  $\mathbb{C}_\infty$  by means of stereographic projection. Here a point on the sphere with coordinates  $(\theta, \phi)$  will be projected to the complex number  $z = \tan\frac{\theta}{2}e^{i\phi}$ , and its antipodal point to  $-1/z^*$ .

We start by considering a unit sphere with coordinates  $X = \sin\theta \cos\phi$ ,  $Y = \sin\theta \sin\phi$  and  $Z = \cos\theta$  centered at the origin of the complex  $XY$ -plane, for which  $Z = 0$ . The idea is to parametrize the cartesian coordinates of the sphere in terms of the coordinate  $z = x + iy$  in the complex plane, so that

$$X = X(x, y), \quad Y = Y(x, y) \quad \text{and} \quad Z = Z(x, y).$$

The cartesian coordinates are

$$X = \frac{2x}{1+r^2}, \quad Y = \frac{2y}{1+r^2} \quad \text{and} \quad Z = \frac{1-r^2}{1+r^2} \quad (2.3)$$

with  $x^2 + y^2 = r^2$ , and with

$$X^2 + Y^2 + Z^2 = \frac{(2x)^2 + (2y)^2 + [1 - (x^2 + y^2)]^2}{(1 + x^2 + y^2)^2} = 1 \quad (2.4)$$

as required for a unit sphere. A projection from the Bloch sphere, minus the point at the south pole, onto the equatorial complex plane  $Z = 0$  which we identify with

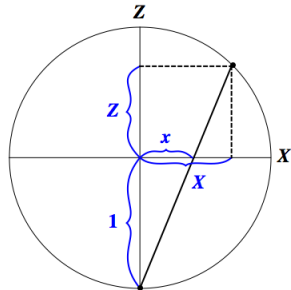


Figure 2.1: Stereographic projection in the XZ-plane.

the complex plane by  $z = x + iy$ , is given by the conformal map

$$f : S^2 \rightarrow \mathbb{C}$$

$$f(X, Y, Z) = \left( \frac{X}{1+Z}, \frac{Y}{1+Z} \right) = (x, y) \quad (2.5)$$

$$f^{-1}(x, y) = \left( \frac{2x}{1+r^2}, \frac{2y}{1+r^2}, \frac{1-r^2}{1+r^2} \right) = (X, Y, Z). \quad (2.6)$$

It is now possible to define the stereographic projection in terms of spherical coordinates

$$z = x + iy = \frac{X + iY}{1 - Z} = \tan \frac{\theta}{2} e^{i\phi}. \quad (2.7)$$

The metric is given by

$$ds^2 = dX^2 + dY^2 + dZ^2 = \frac{4}{(1+r^2)^2} dz^2, \quad (2.8)$$

where  $X^2 + Y^2 + Z^2 = 1$ . This is the Fubini-Study metric, or Fubini-Study distance, which has a physical interpretation of the statistical distance between quantum states. The Fubini-Study distance can be regarded as the length of the geodesic curve connecting two arbitrarily chosen points corresponding to two states.

The general expression for a state is

$$|\psi\rangle = \sum_{k=0}^n Z_k |e_k\rangle = [Z_0; Z_1; \dots; Z_n], \quad (2.9)$$

where  $\{|e_k\rangle\}$  is a set of orthonormal basis vectors for the Hilbert space and  $Z_k = [Z_0; Z_1; \dots; Z_n]$  is the standard notation for a point in the projective space  $\mathbb{CP}^n$  in homogeneous coordinates. Homogeneous coordinates  $[Z_0; Z_1; \dots; Z_n]$ , or projective coordinates, are a system of coordinates used in projective geometry. In this system geometric objects can be given a representation as elements based on  $[Z_0; Z_1; \dots; Z_n]$ .

As long as not all  $Z_0, Z_1, \dots, Z_n$  are equal to zero, any point in the projective space can be represented by  $[Z_0; Z_1; \dots; Z_n]$ . Then, given two points  $|\psi\rangle = Z_k$  and  $|\phi\rangle = W_k$  in the  $N$ -dimensional projective space  $\mathbb{C}\mathbf{P}^{N-1}$ , the Fubini-Study distance between them is defined as

$$D_{\text{FS}} = \arccos \sqrt{\frac{|\langle \psi | \phi \rangle|^2}{\langle \psi | \psi \rangle \langle \phi | \phi \rangle}} = \arccos \sqrt{\frac{Z_\alpha \bar{W}^\alpha W_\beta \bar{Z}^\beta}{Z_\alpha \bar{Z}^\alpha W_\beta \bar{W}^\beta}}. \quad (2.10)$$

Here  $\bar{Z}_\alpha$  is the complex conjugate of  $Z^\alpha$ . To treat the case when  $|\psi_2\rangle = 0$  we have to extend the complex plane  $\mathbb{C}$  by adding a point at infinity. The obtained set  $\mathbb{C} \cup \{\infty\} = \mathbb{C}_\infty$  is the aforementioned extended complex plane. Consequently there is a one-to-one mapping between all points  $z$  in the extended complex plane and the Bloch sphere.

### Visualizing the State Space in Higher Dimensions

Our state space may be viewed as a complex projective space if the number of dimensions of the Hilbert space is finite. Then a pure state in the  $N$ -dimensional Hilbert space  $\mathcal{H}_N$ , described by a vector  $|\psi\rangle$  in  $\mathbb{C}^N$ , is also a point in the projective space  $\mathbb{C}\mathbf{P}^{N-1}$ . The standard convention is to assume that  $|\psi\rangle = Z_0|0\rangle + Z_1|1\rangle + \dots + Z_{N-1}|N-1\rangle$  is a unit vector and ignore its global phase. For  $Z_0 \neq 0$  we have an equivalence relation

$$|\psi\rangle \sim n_0|0\rangle + n_1 e^{i\phi_1}|1\rangle \dots + n_{N-1} e^{i\phi_{N-1}}|N-1\rangle,$$

where  $n_i \geq 0$  and  $n_0^2 + n_1^2 + \dots + n_{N-1}^2 = 1$ . One can think of each equivalence class as a complex line through the origin in  $\mathbb{C}^N$ , or a complex one-dimensional subspace. These subspaces form a complex projective space  $\mathbb{C}\mathbf{P}^{N-1}$ , where the superscript  $N-1 = n$  stands for the complex dimension of the space. Thus there is a one-to-one correspondence between points in  $\mathbb{C}\mathbf{P}^{N-1}$  and physical states of an  $N$ -level quantum system.

Consider the case of  $N = 2$ , whence a pure state is a point in  $\mathbb{C}\mathbf{P}^1$ . Ignoring the global phase and normalization factor, the state becomes

$$\begin{aligned} |\psi\rangle &= n_0|0\rangle + n_1 e^{i\phi_1}|1\rangle \\ &= \cos \frac{\theta}{2} |0\rangle + e^{i\phi} \sin \frac{\theta}{2} |1\rangle, \end{aligned} \quad (2.11)$$

which equals (2.2) and where  $0 \leq \theta < \pi$  and  $0 \leq \phi < 2\pi$  are the normal spherical coordinates. As earlier stated, the set of all such vectors constitute the Bloch sphere. In other words, for  $N = 2$  the corresponding projective space  $\mathbb{C}\mathbf{P}^1$  is equal to a sphere.

It is difficult to visualize  $\mathbb{C}\mathbf{P}^n$  in higher dimensions, since it no longer has the form of a sphere. Already for  $n = 2$  the visualization of the projective complex

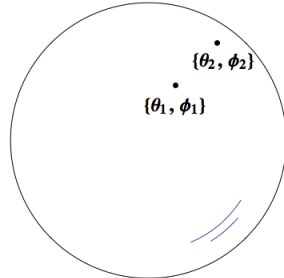


Figure 2.2: Visualization of the projective space  $\mathbb{C}\mathbf{P}^2$

space becomes much more complicated. In this case  $\mathbb{C}\mathbf{P}^2$  corresponds to the space of complex lines through the origin in  $\mathbb{C}^3$ .

However, it is possible to visualize  $\mathbb{C}\mathbf{P}^n$  in real terms by means of the stellar representation. The idea is then that vectors in  $\mathbb{C}\mathbf{P}^{n+1}$  are in one-to-one correspondence with the set of  $n$ th degree polynomials, which in turn can be represented by points on a sphere. This will be explained in next section.

## 2.2 The Stellar Representation

In this section we present the relation between vectors in the state space and points on a sphere, i.e. we show that we may regard points in the complex projective space  $\mathbb{C}\mathbf{P}^n$  as unordered sets of  $n = N - 1$  points on a Bloch sphere [2–4]. By analogy, this is similar to stars on a celestial sphere, and hence the points are sometimes called stars. Therefore this relation is called the stellar representation, also known as the Majorana representation.

We derive the polynomial associated with each vector in a simple example, discuss how this is related to a rotation operator and describe the context in which a rotation of the state vector corresponds to a rotation of the sphere. Of particular interest to us are the coherent states, which correspond to coinciding stars on the sphere, and the maximally non-coherent states, which we will try to define as stars that are as spread out as possible. We will, however, not be able to deal with these very effectively until we reach Chapter 3 and Chapter 4, in which we describe the coherent states and non-coherent states respectively.

### State Vector Polynomial

Let us associate a polynomial to each vector in  $\mathbb{C}^{n+1}$ , and the roots of that polynomial to the corresponding point in  $\mathbb{C}\mathbf{P}^n$ . The roots are the stars on the celestial sphere. The idea is that there is a one-to-one correspondence between vectors in

$\mathbb{C}^{n+1}$  and the set of  $n$ th degree polynomials in one complex variable  $z$  by setting

$$p(z) = Z_n z^n + Z_1 z^{n-1} + \dots + Z_0. \quad (2.12)$$

By rescaling the vector  $Z^k$  so that  $Z_n = 1$ , we see that the points in  $\mathbb{C}\mathbf{P}^n$  will be in one-to-one correspondence with unordered sets of  $n$  complex numbers, namely with the complex roots  $w_1, w_2, \dots, w_n$  of the polynomial

$$\begin{aligned} p(z) &= Z_n z^n + Z_{n-1} z^{n-1} + \dots + Z_1 z^1 + Z_0 \\ &= Z_n (z - w_n) \cdot (z - w_2) \cdot \dots \cdot (z - w_n). \end{aligned} \quad (2.13)$$

The complex roots  $w_1, \dots, w_n$  of the polynomial can be represented as sets of  $n$  stars on a 2-sphere through stereographic projection. Degenerate roots are allowed, and if  $Z_0 = 0$  then infinity counts as a root.

We regard points in the complex projective space  $\mathbb{C}\mathbf{P}^n$  as quantum states. Distances and areas in  $\mathbb{C}\mathbf{P}^n$  are invariant under only certain projective transformations, namely the unitary transformations. Since the phase factor is irrelevant, it is enough to study the special unitary group  $SU(N)$ . By doing so, we may restrict the transformations acting on the 2-sphere to the distance preserving subgroup  $SU(2)/\mathbb{Z}_2 = SO(3)$ . The next step is to show that an  $SU(2)$ -transformation corresponds to an ordinary rotation of the sphere upon which we have placed our stars.

### **$SU(2)$ -Transformation**

We represent a state that is an eigenstate of  $\mathbf{n} \cdot \mathbf{L}$  with eigenvalue  $m$  by  $j + m$  points at the point where  $\mathbf{n}$  meets the sphere, and  $j - m$  points at the antipode. In this case a state of spin 'up' in the direction given by the unit vector  $\mathbf{n}$  is represented by  $n = 2j$  points at the point where  $\mathbf{n}$  meets the sphere.  $\mathbf{L}$  is the orbital angular momentum.

Let us study the rotation of the state by  $L_x$  in a simple example. Consider a spin  $j = 1$  particle and place two points at the positive intersection between the  $x$ -axis and the sphere, the so-called 'east pole', for which  $\theta = \frac{\pi}{2}$  and  $\phi = 0$ . The polynomial in this example is given by

$$p(z) = aZ_2 z^2 + bZ_1 z + cZ_0. \quad (2.14)$$

In stereographic coordinates the east pole is at  $z = 1$ . The east pole polynomial then becomes

$$p(z) = (z - 1)^2 = z^2 - 2z + 1. \quad (2.15)$$

The eigenvector of  $L_x$  with eigenvalue  $+1$  is  $Z_k = (1, \sqrt{2}, 1)$ . If this is to equal (2.15),



we must choose conventions for the coefficients of the polynomial as following:

$$\begin{aligned} p(z) &= z^2 - 2z + 1 \\ &\equiv Z_2 z^2 - \sqrt{2} Z_1 z + Z_0 \\ &\Rightarrow \begin{cases} Z_0 = 1 \\ Z_1 = \sqrt{2} \\ Z_2 = 1. \end{cases} \end{aligned}$$

Computing rotations by  $L_y$  and  $L_z$  yield the same results. After similar calculations we see that to any point in  $\mathbb{CP}^n$ , given by the homogeneous coordinates  $Z_k$ , we want to associate the  $n + 1$  unordered roots of the polynomial

$$p(z) \equiv \sum_{k=0}^n (-1)^k Z_k \sqrt{\binom{n}{k}} z^{n-k}. \quad (2.16)$$

Thus if we apply a rotation operator to a point in  $\mathbb{CP}^n$ , the effect is a rotation of the sphere containing the  $n$  points by the angle  $\theta$  around the axis directed along the vector  $(\sin \phi, \cos \phi, 0)$  normal to the  $z$ -axis and to the vector  $\mathbf{n}$ . This implies that the action of the  $SU(2)$ -matrix upon the state vector  $|\psi\rangle = [Z^0, \dots, Z^n]^T$  given by  $SU(2)|\psi\rangle$  is the same as a rotation of the stars on the celestial sphere. Note that the conventions for the coefficients of the polynomial have been adjusted so that it corresponds to the desired rotations.

We have thereby arrived at the stellar representation, in which points in  $\mathbb{CP}^n$  are represented by  $n$  unordered stars on a sphere. A state for which the  $n$  roots of the polynomial are equal is called a coherent state, which we will discuss in the next chapter.



## Chapter 3

# Coherent States

The main purpose of our investigation is to maximize the Wehrl entropy. To this end we study coherent states and their properties. We first introduce the canonical coherent states and some of their properties and thereafter define the Bloch coherent states analogously. The material presented here can be found in Ref. [1, 6, 7].

### 3.1 Canonical Coherent States

In this section we present the canonical coherent states, also known as Glauber coherent states. They are the quantum states whose dynamics most closely resembles the dynamics of classical systems. Some of their most important properties are the following:

- The coherent states saturate the Heisenberg inequality.
- The coherent states are eigenvectors of the annihilation operator.
- The coherent states are obtained from the ground state by a unitary action of the Heisenberg-Wehl group and may thus be regarded as an orbit.
- The coherent states are complete in the sense that any state can be obtained by superposing coherent states. They constitute an overcomplete set because they are much more numerous than the elements of an orthonormal set would be, and are therefore not orthogonal and do overlap.
- The coherent states resolve the identity operator.

Consider a Hilbert space  $\mathcal{H}$  with position and momentum operator given by  $\hat{q}$  and  $\hat{p}$  respectively. The Heisenberg algebra of the operators is defined by  $[\hat{q}, \hat{p}] = i\hbar\mathbf{1}$ , where  $\hbar$  is the Planck constant and  $\mathbf{1}$  the identity operator. From now on we set  $\hbar = 1$  and rescale the operators  $\hat{q}$  and  $\hat{p}$  so that they are dimensionless. The

position and momentum operators can be expressed in terms of the annihilation and creation operators  $a$  and  $a^\dagger$  of the harmonic oscillator:

$$\hat{q} = \frac{1}{\sqrt{2}}(a + a^\dagger), \quad \hat{p} = -\frac{i}{\sqrt{2}}(a - a^\dagger).$$

We now introduce minimum-uncertainty states, which are states that saturate the Heisenberg inequality

$$(\Delta\hat{q})(\Delta\hat{p}) \geq \frac{1}{2}, \quad (3.1)$$

where the variance is given by the square of uncertainty  $(\Delta\hat{X})^2 = \langle z|X^2 - \langle X\rangle^2|z\rangle$  with  $\langle X\rangle = \langle z|X|z\rangle$ . This inequality is saturated by coherent states and squeezed states, which may be regarded as the 'least quantum' or 'most classical' quantum states.

Coherent states are minimum-uncertainty states with variances equal to those of the vacuum state, i.e. their product equals the minimum value allowed by the Heisenberg uncertainty principle. In this case the uncertainty in position and momentum form a circular uncertainty region in phase space.

Squeezed states [9] are a general class of minimum-uncertainty states. A state is said to be squeezed if one of its variances become smaller than the square root of the minimum-uncertainty product. The uncertainty in position and momentum for squeezed state form an elliptic uncertainty region in phase space.

The states which are the closest to classical states are those that not only saturate the uncertainty relation, but also for which the uncertainty of position and momentum are equal, i.e. form a circular region in phase space. This is true for coherent states, but not for squeezed states. Thus coherent states are the most classical quantum states.

In Chapter 4 we will introduce the Wehrl entropy, which presents a good measure of how much 'coherence' a given state has. The Wehrl entropy can be regarded as a classicality measure, and attains its minimum for coherent states.

### Heisenberg-Weyl Group

The canonical coherent states form a subset of states that can be reached from a special reference state through transformations belonging to the Heisenberg-Weyl group. In other words they constitute an orbit under the action of the Heisenberg-Weyl group. This group acts irreducibly on the Hilbert space, which is infinite dimensional for the canonical coherent states, unlike the Hilbert space for the Bloch coherent states which is finite dimensional.

Let us form the unitary group elements  $\hat{U}(p, q) = e^{i(p\hat{q} - q\hat{p})}$  and define the vacuum state  $|0\rangle$  as the state that is annihilated by  $\hat{a}$ . The canonical coherent states are defined as  $|p, q\rangle = \hat{U}(p, q)|0\rangle$ , with the vacuum state serving as the reference state and where  $q$  and  $p$  are coordinates on the space of coherent states. Then the set of coherent states can be viewed as an orbit obtained from the ground state  $|0\rangle$

by means of a unitary group action. Bloch coherent states can be defined in an analogous way (see Section 3.2).

Let us trade  $\hat{q}$  and  $\hat{p}$  for the creation and annihilation operators. Using the formula

$$\exp(\hat{A}) \exp(\hat{B}) = \exp\left(\frac{1}{2}[\hat{A}, \hat{B}]\right) \exp(\hat{A} + \hat{B}) = \exp([\hat{A}, \hat{B}]) \exp(\hat{B}) \exp(\hat{A}),$$

which is valid whenever  $[\hat{A}, \hat{B}]$  commutes with  $\hat{A}$  and  $\hat{B}$ , and defining the complex coordinate

$$z = \frac{1}{\sqrt{2}}(q + ip), \quad (3.2)$$

the coherent states can be expressed as

$$|p, q\rangle = |z\rangle = e^{za^\dagger - \bar{z}a}|0\rangle. \quad (3.3)$$

The coherent state  $|z\rangle$  is an eigenvector of the annihilation operator  $a$  with eigenvalue  $z$ ,

$$a|z\rangle = z|z\rangle, \quad (3.4)$$

and with  $\langle z|a^\dagger = \bar{z}\langle z|$ . From this equation follows that  $f(a)|z\rangle = f(z)|z\rangle$  for an analytic function  $f$ . This is known as the Fock-Bargmann representation, which is a projection of a state  $|\psi\rangle$  onto the coherent states  $|z\rangle$ . It is defined as the scalar product of the normalized vector  $|\psi\rangle = \sum_{n=0}^{\infty} c_n |n\rangle$  in the Hilbert space with the coherent states  $|z\rangle = e^{-\frac{|z|^2}{2}} \sum_{n=0}^{\infty} \frac{z^n}{\sqrt{n!}} |n\rangle$ , namely

$$\begin{aligned} \langle \bar{z}|\psi\rangle &= \phi(z) \equiv e^{-\frac{|z|^2}{2}} \sum_{n=0}^{\infty} c_n \frac{\bar{z}^n}{\sqrt{n!}} \\ &= e^{-\frac{|z|^2}{2}} \sum_{n=0}^{\infty} c_n f_n(\bar{z}) \\ &= e^{-\frac{|z|^2}{2}} \psi(\bar{z}) \end{aligned} \quad (3.5)$$

where  $f_n(z) = \frac{z^n}{\sqrt{n!}}$  and  $\{|n\rangle\}$  are the Fock number states.

### Resolution of Identity

There are two important facts which follow from the irreducibility of the group representation of coherent states. The first is that the coherent states are complete in the sense that any state can be obtained by superposing coherent states. In fact they form an overcomplete set, which means that there are at least two of the states in the family that are not linearly independent.

Second, the coherent states satisfy the resolution of the identity given by

$$\frac{1}{\pi} \int d^2z |z\rangle\langle z| = \frac{1}{2\pi} \int dq dp |q, p\rangle\langle q, p| = \sum_{i=0}^{\infty} |e_i\rangle\langle e_i| = \mathbf{1}. \quad (3.6)$$

Note that (3.6) is similar to the completeness relation  $\sum_{i=1}^N |e_i\rangle\langle e_i| = \mathbf{1}$ ,  $\langle e_i|e_j\rangle = \delta_{ij}$ , for an orthonormal basis, in which the sum has been replaced by an integral over the phase space. Apart from an overall numerical factor, (3.6) follows from the fact that the operator on the left-hand side commutes with the Heisenberg-Weyl group element  $\hat{U}(p, q)$ .

### 3.2 Bloch Coherent States

In this section we derive the Bloch coherent states, also known as spin coherent states, similar to how we derived the canonical coherent states, but with the  $SU(2)$  group instead of the Heisenberg-Weyl group. We show that Bloch coherent states are constructed utilizing the standard representation of angular momentum operators and the unitary irreducible representation of the rotation group  $SU(2)$ . Our Hilbert space will be any finite-dimensional Hilbert space in which  $SU(2)$  acts irreducibly.

Consider a spin system of fixed total angular momentum  $j$ ,  $j = 0, \frac{1}{2}, 1, \frac{3}{2}, \dots$ . Let  $J = (J_x, J_y, J_z)$  denote the usual angular momentum operators with cyclic commutation relations  $[J_x, J_y] = iJ_z$ ,  $[J_y, J_z] = iJ_x$  and  $[J_z, J_x] = iJ_y$  where  $\hbar = 1$ . We select the basis vectors  $|j, m\rangle$  as eigenvectors of the commuting pair of operators  $J^2 = J_x^2 + J_y^2 + J_z^2$  and  $J_z$ . Then the angular momentum eigenstates of  $J^2$  and  $J_z$  are defined by

$$J^2|j, m\rangle = j(j+1)|j, m\rangle$$

$$\text{and } J_z|j, m\rangle = m|j, m\rangle,$$

where  $m = -j, -j+1, \dots, j-1, j$ . The angular momentum eigenstates  $|j, m\rangle$ , also known as the Dicke states, form an orthonormal basis in the Hilbert space  $\mathcal{H}_N$ , with the quantum number  $m$  interpreted as half the difference between the number of excited and unexcited spins. The eigenvalues  $j(j+1)$  of the operator  $J^2$  determine the dimension  $N = n+1 = 2j+1$  of  $\mathcal{H}_N$ , with  $n$  being the total number of spins. For  $n = 2j$ , the physical system may be regarded as a collection of  $n$  two-level atoms instead of a spin system of total spin  $j$ .

The raising and lowering operator  $J_{\pm} = J_x \pm iJ_y$  act on the basis through

$$J_+|j, m\rangle = \sqrt{[(j-m)(j+m+1)]}|j, m+1\rangle$$

$$\text{and } J_-|j, m\rangle = \sqrt{[(j+m)(j-m+1)]}|j, m-1\rangle.$$

Here the highest excited state  $|j, j\rangle$  and the ground state  $|j, -j\rangle$  are defined by  $J_+|j, j\rangle = 0$  and  $J_-|j, -j\rangle = 0$  respectively. These operators together with  $J_z$  are generators of the rotational group  $SU(2)$ .

As stated above, the canonical coherent states form an orbit under the action of the Heisenberg-Weyl group. In a similar way the set of Bloch coherent states is an orbit under the action of the  $SU(2)$  group. By choosing the reference state  $|j, j\rangle$ , which has spin up along the  $z$ -axis, the set of Bloch coherent states become

states of the form  $\mathcal{D}|j, j\rangle$ , where  $\mathcal{D}$  is the Wigner rotation matrix. The reference state is described by the vector  $[1, 0, 0, \dots]$  when using the standard representation of the angular momentum operators (Appendix A). Then the coherent states are described by the first column of  $\mathcal{D}$ .

Let us choose the following parametrization for the rotation operator:

$$\mathcal{D} = e^{zJ_-} e^{-\ln(1+|z|^2)J_z} e^{-\bar{z}J_+} e^{i\tau J_z}. \quad (3.7)$$

With this parametrization the coherent states may be expressed as

$$|z\rangle = \mathcal{D}|j, j\rangle = e^{zJ_-} e^{-\ln(1+|z|^2)J_z} e^{-\bar{z}J_+} e^{i\tau J_z} |j, j\rangle. \quad (3.8)$$

We can prove this statement using  $2 \times 2$  matrices, and it will be true for all representations. Note that (3.7) is a general  $SU(2)$ -matrix, with the complex number  $z$  being a stereographic coordinate on the sphere. Since the Wigner matrix is a representation of the  $SU(2)$  group, it rotates the quantum mechanical states it acts upon.

Our reference state  $|j, j\rangle$  is a fixed point in  $\mathbb{C}\mathbb{P}^n$  under transformations of  $e^{i\tau J_z}$ , so when the factor  $e^{i\tau J_z}$  acts on  $|j, j\rangle$  the only contribution to the coherent states is that of an overall constant phase. We choose this overall phase to be zero. Using the Pauli matrices in Appendix A, (3.8) can be written

$$|z\rangle = \frac{1}{(1+|z|^2)^j} e^{zJ_-} |j, j\rangle. \quad (3.9)$$

Since the reference state is annihilated by  $J_+$ , the complex conjugate  $\bar{z}$  only enters the expression for coherent states in the normalization factor. Taking into account that the ladder operator  $J_-$  is a lower triangular matrix, it is straightforward to express the coherent state in component form. To show this we use the series expansion for the matrix exponential

$$e^{zJ_-} = \sum_{k=0}^{\infty} \frac{(zJ_-)^k}{k!} = \sum_{m=-j}^j \frac{z^{m+j}}{(m+j)!} J_-^{m+j} \quad (3.10)$$

together with the recursion relation

$$J_-^{j+m} |j, -j\rangle = \sqrt{\frac{(2j)!}{(j-m)!}} \sqrt{(j+m)!} |j, m\rangle \quad (3.11)$$

which yields the following expression for the coherent states

$$|z\rangle = \sum_{m=-j}^j \frac{z^{m+j}}{(1+|z|^2)^j} \sqrt{\binom{2j}{j+m}} |j, m\rangle. \quad (3.12)$$

Using  $z = \tan \frac{\theta}{2} e^{i\phi}$  a coherent spin state can be written in terms of the angles  $\theta$  and  $\phi$  in the standard spherical coordinate system

$$|z\rangle = |\theta, \phi\rangle \equiv \sum_{k=0}^n |k\rangle \sqrt{\binom{n}{k}} \left(\cos \frac{\theta}{2}\right)^{n-k} \left(\sin \frac{\theta}{2} e^{i\phi}\right)^k. \quad (3.13)$$

Ignoring the normalization factor, the non-normalized homogenous coordinates are given by

$$Z^k = (1, \sqrt{2j}z, \dots, \sqrt{\binom{2j}{j+m}} z^{j+m}, \dots, z^{2j}).$$

### Resolution of Identity

One of the requirements for coherent states is that there should exist a resolution of identity, so that an arbitrary state can be expressed as a linear combination of coherent states. This must be true also for Bloch coherent states, for which the resolution of identity is

$$(2j+1) \int \frac{d\Omega}{4\pi} |z\rangle \langle z| = \sum_{m=-j}^j |j, m\rangle \langle j, m| = \mathbf{1} \quad (3.14)$$

with the rotationally invariant measure given by

$$d\Omega = \sin \theta \, d\theta \, d\phi = \frac{4r \, dr \, d\phi}{(1+r^2)^2}, \quad (3.15)$$

where we have used polar coordinates  $z = r e^{i\phi}$ . To show this, we rewrite the coherent states for  $z = r e^{i\phi}$ ,

$$|z\rangle = \sum_{m=-j}^j \frac{r^{m+j} e^{i\phi(j+m)}}{(1+r^2)^j} \sqrt{\binom{2j}{j+m}} |j, m\rangle, \quad (3.16)$$

and use the fact that the integral of the complex exponential becomes a Dirac delta. After shifting the index in the summation so that it starts from zero and setting  $j+m=k$ , we find that the summation factor equals one, that is

$$\sum_{k=0}^{2j} \binom{2j}{k} \frac{r^{2k}}{(1+r^2)^{2j}} = \frac{(1+r^2)^{2j}}{(1+r^2)^{2j}} = 1. \quad (3.17)$$

Inserting this result into (3.14) gives the resolution of identity.

We also require that coherent states saturate an uncertainty relation such as

$$j \leq \Delta^2 \leq j(j+1). \quad (3.18)$$



Here  $\Delta^2$  is a measure for uncertainty

$$\Delta^2 = (\Delta J_x)^2 + (\Delta J_y)^2 + (\Delta J_z)^2 = \langle J^2 \rangle - \langle J_i \rangle \langle J_i \rangle, \quad (3.19)$$

which is invariant under  $SU(2)$  and takes the same value for all states in a given  $SU(2)$  orbit in the Hilbert space. The generators  $\hat{J}_i$  are given by the classical phase space functions

$$J_i(\theta, \phi) = \langle z | J_i | z \rangle = j n_i(\theta, \phi) \quad (3.20)$$

for which  $n_i(\theta, \phi)$  is a unit vector pointing in the direction labelled by the angles  $(\theta, \phi)$ . One can prove that the lower bound in (3.18) is saturated only for Bloch coherent states [13].

Recall that the idea in Section 2.2 was to associate a polynomial to each vector in the complex space  $\mathbb{C}\mathbf{P}^n$  and regard the roots of that polynomial as unordered sets of  $n+1$  stars on a sphere through the stellar representation. In this representation Bloch coherent states are distinguished by being the only states for which all stars are located in a single point.



## Chapter 4

# Wehrl Entropy

In this chapter we present states corresponding to spherical arrangements of points that maximize the Wehrl entropy. To find these arrangements we introduce the Husimi  $Q$ -function following Refs. [1, 15, 16], explain how it allows us to reconstruct the quantum states through their overlaps with the set of coherent states, and discuss some of its geometrical properties. We present the Wehrl entropy in terms of the Husimi function and give a short description of the Lieb conjecture [15], which states that the Wehrl entropy attains its minimum for coherent states. We describe the problem of distributing points on a sphere in order to optimize some function depending on the positions of the points, and identify the configurations for which local maxima of the Wehrl entropy occur. Furthermore, using part of the proof of the Lieb conjecture [25], we give a geometric illustration of how quantum channels for coherent states majorize all other quantum channels.

### 4.1 Husimi Function

The attempts to find a description of quantum states that are similar to classical states have given rise to several functions in phase space, such as the Wigner function and the Husimi function. These functions allow for the representation of quantum states by quasiprobability distributions in phase space.

The Wigner function permits a direct comparison between classical and quantum dynamics. In the case of coherent states as well as for squeezed states, the Wigner function takes the form of a Gaussian. Generally, however, it is not a positive function and therefore not a probability distribution, even though it is normalized.

To overcome this shortcoming the Husimi  $Q$ -function is introduced, which is defined in a way that guarantees it to be non-negative and gives it a probability interpretation. The Husimi function is a smoothed Wigner function with high frequency behavior suppressed. Unlike classical probability distributions, it is bounded

from above. We will study the  $Q$ -function for the  $SO(3)/SO(2) = \mathbf{S}^2$  orbit, i.e. the Bloch coherent states.

We start by presenting the Bargmann function. Consider a Hilbert space  $\mathcal{H}_N$  of dimension  $N = n + 1 = 2j + 1$  with basis states  $|e_k\rangle = |j, m\rangle$ . A general pure state in  $\mathcal{H}_N$  can be written in the form

$$|\psi\rangle = \sum_{k=0}^n Z_k |e_k\rangle \quad (4.1)$$

and a normalized Bloch coherent state in the form

$$|z\rangle = \frac{1}{(1 + |z|^2)^{n/2}} \sum_{k=0}^n \sqrt{\binom{n}{k}} z^k |e_k\rangle. \quad (4.2)$$

Here  $Z_k$  is a component of a normalized vector and  $z^k$  is the complex number  $z = \tan \frac{\theta}{2} e^{i\phi}$  raised to the power  $k$ .

We now introduce the Bargmann function

$$\psi(z) = \langle \psi | z \rangle = \frac{1}{(1 + |z|^2)^{n/2}} \sum_{k=0}^n \bar{Z}_k \sqrt{\binom{n}{k}} z^k, \quad (4.3)$$

which is defined as the overlap of a state with the set of coherent states. Note that this is (up to a factor) an  $n$ th order polynomial uniquely associated to any state. As a result it can be factorized

$$\psi(z) = \frac{\bar{Z}_n}{(1 + |z|^2)^{n/2}} (z - \omega_1)(z - \omega_2) \dots (z - \omega_n). \quad (4.4)$$

In Section 2.2 we discussed the correspondence between the state vector polynomial  $p(z) = Z_n(z - \omega_1)(z - \omega_2) \dots (z - \omega_n)$  and stars on a sphere. Since the Bargmann function is uniquely characterized by the zeroes  $\omega_i$  of the polynomial (4.4), it can be represented by stars on the celestial sphere. The zeroes of the Bargmann function are always antipodally placed with respect to the stars. In the case of a coherent state  $|z_0\rangle$  the Bargmann function is

$$\psi_{z_0}(z) = \langle z_0 | z \rangle = \frac{\bar{z}_0^n}{(1 + |z|^2)^{n/2} (1 + |z_0|^2)^{n/2}} \left( z + \frac{1}{\bar{z}_0} \right)^n. \quad (4.5)$$

When we compare this to the polynomial  $p(z) = (z - z_0)^n$  describing a coherent state, we find that  $w_0 = -1/\bar{z}_0$ .

We now define the Husimi function for Bloch coherent states as the square of the absolute value of the Bargmann function,

$$\begin{aligned}
Q_\psi(z) &= |\langle \psi | z \rangle|^2 \\
&= \frac{1}{(1 + |z|^2)^n} \left( \sum_k^n \bar{Z}^k \sqrt{\binom{n}{k}} z^k \right) \left( \sum_{k'}^n Z_{k'} \sqrt{\binom{n}{k'}} \bar{z}^{k'} \right) \\
&= \frac{|Z_n|^2}{(1 + |z|^2)^n} |z - w_1|^2 |z - w_2|^2 \dots |z - w_n|^2.
\end{aligned} \tag{4.6}$$

It is clear that  $Q_\psi(z)$  is positive. Furthermore, since the integral of  $Q_\psi(z)$  over phase space equals one,

$$\frac{n+1}{4\pi} \int d\Omega Q_\psi(z) = 1 \tag{4.7}$$

it provides a genuine probability distribution on the sphere. This can be shown by inserting the square of (4.3) into (4.7) and expressing  $z$  in complex polar coordinates  $z = re^{i\phi}$  (cf. (3.16)).

The Husimi function is bounded from above. Its maximum value determines the minimum distance between  $|\psi\rangle$  and the orbit of coherent states  $|z\rangle$ . This is given by the Fubini-Study distance between  $|\psi\rangle$  and  $|z\rangle$ ,  $D_{\text{FS}} = \arccos \sqrt{\kappa}$ , where  $\kappa = |\langle \psi | z \rangle|^2 = Q_\psi(z)$ . The physical interpretation of the Husimi function is as the projection of the wave function  $\psi$  onto coherent states, which are localized in phase space  $(q, p)$  with a minimum product of the uncertainties  $\Delta q, \Delta p$ .

## 4.2 Wehrl Entropy

In this section we finally present the Wehrl entropy. We define it for the Husimi  $Q$ -function and give a short description of the Lieb conjecture, which was recently proved by Lieb and Solovej [25]. The Lieb conjecture states that the Wehrl entropy attains its global minimum for Bloch coherent states.

### Lieb Conjecture

The concept 'entropy' was created by Rudolf Clausius in 1864 [18]. According to Clausius, the entropy change of a system is obtained by an infinitesimal transfer of heat to a closed system driving a reversible process, divided by the equilibrium temperature of the system. The concept of entropy was later clarified by Ludwig Boltzmann, who dealt with the mechanical theory of heat in connection with probabilities.

In information theory, entropy is the average information needed to specify the outcome of a series of experiments for which the outcome is a random variable. The term usually refers to the Shannon entropy

$$S(P) = -k \sum p_i \ln p_i, \tag{4.8}$$

where  $k$  is a positive number that we usually set equal to 1. The Shannon entropy is a function of a probability distribution  $P$  for a finite number  $N$  of possible outcomes, that is, a vector  $\vec{p}$  whose  $N$  components obey  $p_i \geq 0$  and  $\sum_i p_i = 1$ . It can be interpreted as a measure of the uncertainty about the outcome of an experiment that is known to occur according to the probability distribution  $P$ .

The entropy of a quantum system as a natural generalization of the classical entropy was proposed by von Neumann. The quantum entropy, or von Neumann entropy, is the quantum analog of the Shannon entropy that captures both classical and quantum uncertainty in a quantum state. It is defined by

$$S(\rho) = -\text{Tr } \rho \ln \rho = -\sum_{i=1}^N \lambda_i \ln \lambda_i \quad (4.9)$$

where  $\rho = \sum_{i=1}^N \lambda_i |e_i\rangle\langle e_i|$  is a density matrix with eigenvectors  $|e_i\rangle$  and where  $N$  is the rank of  $\rho$ . Hence the von Neumann entropy is the Shannon entropy of the spectrum of  $\rho$ .

Like the Shannon entropy, the von Neumann entropy is interesting due to its appealing properties. Some of its most important properties are

- Positivity: The von Neumann entropy is non-negative for any density operator  $\rho$ .
- Minimum value: The minimum value of the von Neumann entropy is zero, and it occurs when the density operator is a pure state.
- Concavity: The von Neumann entropy is concave in the density operator:

$$S(\rho) \geq \sum_x p_X(x) S(\rho_x)$$

where  $\rho \equiv \sum_x p_X(x) \rho_x$ . The physical interpretation of concavity is the same as for classical entropy, i.e. entropy can never decrease under a mixing operation.

The von Neumann entropy varies from zero for pure states to  $\ln N$  for maximally mixed states. Recall that we regard entropy as a classicality measure, which measures how much 'coherence' a system has. However, the minimum value of the von Neumann entropy is given by a *pure* state, regardless of whether the state is coherent or not. This does not agree with our definition of *coherent* states  $|z\rangle$  as minimum uncertainty states, for which the entropy should attain its minimum. Clearly this is not true for the von Neumann entropy, which is minimized by all pure states.

To solve this problem Wehrl used the coherent states to define a new concept of classical entropy of a quantum state. According to Wehrl, this 'classical' entropy, or Wehrl entropy, of a quantum system is the entropy of the probability distribution

in phase space, corresponding to the  $Q$ -function of a quantum state in terms of coherent states. Wehrl conjectured [20] that the Wehrl entropy is minimized by coherent states, i.e. the states that saturate the Heisenberg uncertainty inequality. In 1978 this was proven by Lieb [15], who showed that the Wehrl entropy attains a minimum value of 1 for canonical coherent states and that a state that minimizes  $S_W$  must be a pure state. At the same time Lieb conjectured that the extension of Wehrl's entropy to Bloch coherent states of all the irreducible  $SU(2)$  spin representations would yield a minimum entropy of  $n/(n+1)$ , where  $n$  is the number of spins in the system.

The Wehrl entropy for Bloch coherent states is defined by

$$S_W(|\psi\rangle\langle\psi|) \equiv -\frac{n+1}{4\pi} \int_{\Omega} d\Omega Q_{\psi}(z) \ln Q_{\psi}(z), \quad (4.10)$$

where  $Q_{\psi}(z)$  is the Husimi function defined in Eq. 4.6. It follows from concavity of  $-x \ln x$  that a minimizing density matrix must be a pure state, i.e.  $\rho = |\psi\rangle\langle\psi|$  for a normalized vector  $|\psi\rangle$ . The generalized Wehrl conjecture, or Lieb conjecture, states that

$$S_W(|\psi\rangle\langle\psi|) \geq \frac{n}{n+1} = \frac{2j}{2j+1} \quad (4.11)$$

with equality if and only if  $|\psi\rangle$  is a coherent state. The bound is trivial for spin  $j = 1/2$ , in which case every state is a Bloch coherent state, but non trivial already for  $j = 1$ .

In 1988 Lee showed [16] that the Wehrl entropy of a coherent spin state is a local minimum and thereby partially confirmed the Lieb conjecture. Lee also introduced a general expression for the Wehrl entropy of an arbitrary maximum total spin state as a finite series expansion in terms of symmetric functions described in (4.14), which we will use to calculate the *local* maxima of  $S_W$ .

In 1999, eleven years later, Schupp proved [17] the Lieb conjecture for the Wehrl entropy of Bloch coherent states for spin  $j = 1$  and spin  $j = 3/2$ , utilizing a geometric representation of a state of spin  $j$  as  $2j$  points on a sphere. In this representation the Husimi function factorizes into a product of  $2j$  functions, which measures the square chordal distance from the antipode of the point parametrized by  $z$ , to each of the  $2j$  points on the sphere. Schupp used the geometric representation to solve (4.10) for states of arbitrary spin and prove the Lieb conjecture for low spin by actual computation of the entropy.

In 2004 Bodmann showed [21] that the conjecture holds in the limit of large  $n$ , i.e.

$$S_W \geq n \ln \left( 1 + \frac{1}{n+1} \right). \quad (4.12)$$

However, in general the Lieb conjecture remained open for almost 35 years until Lieb and Solovej proved it in 2012 [25]. This will be described further in section 4.6.

We now present the geometric representation of a spin state. Let  $(\theta_i, \phi_i)$  be the direction of a unit vector (the coordinate of a point on the surface of the unit sphere). An arbitrary pure state of an  $n$ -spin system with maximum total spin can be characterized by the locations of  $n$  points on the unit sphere, as presented in Section 2.2. Then a convenient way to rewrite the Husimi function (4.6) is as the product of  $n$  individual distributions

$$Q(z) = k_n \sigma(z, \omega_1) \sigma(z, \omega_2) \dots \sigma(z, \omega_n) \quad (4.13)$$

where  $k_n$  is some normalization factor independent of  $z$  and

$$\sigma(z, \omega) \equiv \frac{|z - \omega|^2}{(1 + |z|^2)(1 + |\omega|^2)} = \frac{1 - \cos d}{2} = \sin^2 \frac{d}{2} = \frac{d_{\text{ch}}^2}{4}, \quad (4.14)$$

for which  $d$  is the geodesic distance and  $d_{\text{ch}}$  is the chordal distance between the two points  $z$  and  $\omega$ . Because of rotational invariance we can assume without loss of

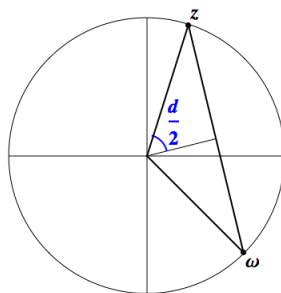


Figure 4.1: Chordal distance between two arbitrary points  $z$  and  $\omega$  on a sphere.

generality that the first point is at the 'north pole' of the sphere,  $\omega = 0$ , and that the second point is parametrized by  $z = \tan \frac{\theta}{2} e^{i\phi}$ . As a result the function  $\sigma(z, \omega)$  can be written

$$\begin{aligned} \sigma(z, \omega) &= \sigma \left( \tan \frac{\theta}{2} e^{i\phi}, 0 \right) \\ &\equiv \frac{|\tan \frac{\theta}{2} e^{i\phi} - 0|^2}{1 + |\tan \frac{\theta}{2} e^{i\phi}|^2} \\ &= \frac{1 - \cos \theta}{2}, \end{aligned}$$

which is one quarter of the square of the chordal distance  $d_{\text{ch}}$  between the two points. We have thereby showed the first part in (4.14), i.e. that  $\sigma(z, \omega) \equiv (1 - \cos d)/2$ . To show the last part in (4.14), that is  $(1 - \cos d)/2 = (d_{\text{ch}}^2)/4$ , we refer to Fig. 4.1. Here simple geometry tells us that  $\sigma(z, \omega)$  is one quarter of the square



of the chordal distance  $d_{\text{ch}}$  between the two points, assuming that the sphere is of unit radius.

In this representation we can now solve the entropy integral (4.10) for all spins, essentially because the logarithm breaks up into a sum of symmetric functions. In effect

$$S_W(|\psi\rangle\langle\psi|) \equiv -\frac{n+1}{4\pi} \int_{\Omega} d\Omega Q(z) \left( \ln k_n + \sum_{i=1}^n \ln(\sigma(z, \omega_i)) \right), \quad (4.15)$$

where we have expressed  $S_W$  in terms of symmetric functions  $k_n$  and  $\sigma(z, \omega_i)$  of the squares of the chordal distance, with the function  $\sigma(\omega_i, \omega_j)$  given by

$$\sigma_{ij} \equiv \sigma(\omega_i, \omega_j) = \frac{|\omega_i - \omega_j|^2}{(1 + |\omega_i|^2)(1 + |\omega_j|^2)}. \quad (4.16)$$

In the particular case of a coherent state, the  $n$  roots of its state vector polynomial are identical, so the  $n$  points on the unit sphere in the geometric representation coincide. This in turn implies that  $\sigma_{ij} = 0$  for any pair of unit vectors, whereupon the Wehrl entropy equals  $S_W = n/(n+1)$ . This agrees with the Lieb conjecture, that is  $S_W = n/(n+1)$  when all the  $n$  roots of its probability  $Q$ -function are identical, i.e. the  $n$  points on the unit sphere coincide.

The following question now arises: what happens when we perturb the system, so that the  $n$  points on the unit sphere spread out a little? To answer that we study the Husimi function for the Dicke states  $|\psi_k\rangle$  (Section 3.2), which are states that have a single component  $Z_k = 1$  and all others equal to zero. In this case the Husimi function is

$$Q_{|\psi_k\rangle}(z) = \binom{n}{k} \frac{|z|^{2k}}{(1 + |z|^2)^n} = \binom{n}{k} \left( \cos \frac{\theta}{2} \right)^{2(n-k)} \left( \sin \frac{\theta}{2} \right)^{2k} \quad (4.17)$$

after switching to polar coordinates  $z = \tan \frac{\theta}{2} e^{i\phi}$  and with index  $k = j - m$ . Here the points are placed at the north pole ( $z = 0$ ) and south pole ( $z = \infty$ ) of the sphere respectively. For  $k = 0 \Rightarrow m = j$ , all points coincide at the north pole, which corresponds to a coherent state. For even  $n$  and  $k = n/2 \Rightarrow m = 0$ , the function is concentrated in a band along the equator. Consequently the Husimi function tends to be more spread out the more non-coherent a state is.

In the upcoming sections we discuss how this affects the Wehrl entropy. We show that the Wehrl entropy increases as the points on the sphere spread further apart and attains a maximum for the most non-coherent states, i.e. when the points on the unit sphere are as far as possible from one another. We define the states for which the Wehrl entropy attains a maximum as the 'most quantum' states. Our basic problem, i.e. maximizing the Wehrl entropy, then consists of distributing points on a sphere in order to optimize some function (the Wehrl entropy) which depends on the positions of the points. Note that the distribution of points that corresponds to an optimized value of the function may not be unique, even though the criterion that the points are as far as possible from one another remains.

### 4.3 Problem Description

In this section we describe the problem of distributing points on a sphere in order to optimize some function depending on the positions of the points. Given a number of points  $n$ , our basic problem is to choose the unique spherical arrangement of  $n$  points on the unit sphere determined by extremal values of some function of the arrangement. Examples of such functions are described in classical problems such as the Thomson problem [22] and the Toth problem [23]. In order to find the spherical arrangements that maximize the Wehrl entropy we study the configurations that solve the functions described in the Thomson problem, the Toth problem and in the article [24] 'Quantifying Quantumness and the Quest for Queens of Quantum' (QQ), and investigate if these give local maxima to the Wehrl Entropy. Our method of solution is based on computer supported analytical calculations and intelligent estimations.

If we want to place  $n$  points on the circumference of a circle so that they are as far away from each other as possible, we should place them at the vertices of a regular  $n$ -gon. The platonic solids are three dimensional analogues of regular polygons and thus it is natural to conjecture that they correspond to optimal configurations for the relevant values of  $n$ . Since we restrict our investigations to 2-9 points, we only consider the tetrahedron, the octahedron and the cube as possible solutions out of the five platonic solids.

A characteristic of optimization problems on the sphere is that they have many local extreme values. Therefore it is usually difficult to prove that a certain arrangement of points gives a global maximum or minimum. This difficulty emerges not only in our solution method, but also in an eventual numerical analysis. Hence we will concentrate our efforts to finding local maxima, i.e. identifying what angles  $\theta$  and  $\phi$  that maximize  $S_W$ . It is however likely that our local maxima also are global maxima.

One could use a purely numerical approach to this optimization problem. Such an analysis would consist of dividing the sphere into a finite number of area elements, making an initial guess of a point in one of the area elements  $(\theta_i, \phi_i)$ , and then vary the positions of the surrounding points until a (local) maximum is found. In theory a search through all configurations of  $\{(\theta_i, \phi_i)\}_{i=1}^n$  could yield more than one maximum, which would falsify the assumption that our estimated maximum is global. The more precise the discretization is, the more values of  $(\theta_i, \phi_i)$  have to be considered, and the longer time the investigation takes. Furthermore, we might still miss a maximum due to a too rough discretization.

We do not consider a numerical analysis of the Wehrl entropy in this thesis.

#### Description of the Thomson, Toth and QQ Problems

In the Thomson problem we consider  $n$  point charges which are confined to the surface of a sphere and interact with each other through Coulomb's inverse square law. The desired distribution is that which minimizes the potential energy. In

the Toth problem,  $n$  points have to be arranged on a sphere so that the minimum pairwise distance becomes maximal. In the QQ article, a quantumness measure defined as the Hilbert-Schmidt distance from the state  $\rho$  to the set of classical states (which is the convex hull of spin coherent states) is introduced in order to quantify how quantum an arbitrary mixed spin- $j$  quantum state  $\rho$  is. The problem in this case consists of optimizing the quantumness measure.

### Defining an expression for the Wehrl Entropy for the angles $\theta_i$ and $\phi_i$ corresponding to $n$ points on the unit sphere

Recall that the Husimi function can be written in terms of symmetric functions  $k_n$  and  $\sigma(z, \omega_i)$  of the squares of the chordal distance, with the function  $\sigma_{ij} = \sigma(\omega_i, \omega_j)$  given by (4.16). By expressing the unit vectors  $\omega_i$  and  $\omega_j$  in stereographic coordinates, we can expand  $\sigma_{ij}$  in terms of  $\theta$  and  $\phi$  as

$$\begin{aligned} \sigma(\omega_i, \omega_j) &= \frac{|\tan \frac{\theta_i}{2} e^{i\phi_i} - \tan \frac{\theta_j}{2} e^{i\phi_j}|^2}{(1 + \tan^2 \frac{\theta_i}{2})(1 + \tan^2 \frac{\theta_j}{2})} \\ &= \frac{1}{2} - \frac{1}{2} \cos \theta_i \cos \theta_j - \frac{1}{2} \sin \theta_i \sin \theta_j \cos(\phi_i - \phi_j). \end{aligned} \quad (4.18)$$

Since the angles are defined as a change  $\Delta x_i$  added to a fixed angle  $x_{i0}$ ,  $x_i = x_{i0} + \Delta x_i$ , we can rewrite (4.18) as

$$\begin{aligned} \sigma(\omega_i, \omega_j) &= \frac{1}{2} - \frac{1}{2} \cos(\theta_{i0} + \Delta\theta_i) \cos(\theta_{j0} + \Delta\theta_j) \\ &\quad - \frac{1}{2} \sin(\theta_{i0} + \Delta\theta_i) \sin(\theta_{j0} + \Delta\theta_j) \cos(\phi_{i0} - \phi_{j0} + \Delta\phi_i - \Delta\phi_j). \end{aligned} \quad (4.19)$$

In order to maximize  $S_W$ , we have to identify the parameters  $\theta_i$ ,  $\phi_i$ ,  $\Delta\theta_i$  and  $\Delta\phi_i$  for the arrangement of  $n$  points on the sphere. The Wehrl entropy (4.10) in polar coordinates is defined as

$$S_W \equiv -\frac{n+1}{4\pi} \int_0^\pi d\theta \sin \theta \int_0^{2\pi} d\phi Q_\rho(\theta, \phi) \ln [Q_\rho(\theta, \phi)] \quad (4.20)$$

for a coherent spin state  $|z\rangle = |\theta, \phi\rangle$  where  $\theta$  and  $\phi$  are two angles in the standard spherical coordinate system. Using the fact that the logarithm factorizes the integral, we can rewrite (4.20) as (cf. (4.15))

$$S_W(|\psi\rangle\langle\psi|) = -\int_0^\pi d\theta \sin \theta \int_0^{2\pi} d\phi Q_\rho(\theta, \phi) \left( \ln k_n + \sum_{i=1}^n \ln [\sigma(\omega_i, \omega_j)] \right). \quad (4.21)$$

Inserting (4.19) into (4.21) yields an expression for the Wehrl Entropy that depends on the angles  $\theta_i$  and  $\phi_i$  corresponding to  $n$  points on the unit sphere. By evaluating the integrals as in Ref. [16] we obtain the following expression for the Wehrl

entropy<sup>1</sup>

$$S_N = K_N \left[ \sum_{m=0}^{\lfloor N/2 \rfloor} (-1)^m \frac{(N-m)!}{N!} \left( \sum_{l=N-m+1}^{N+1} \frac{N}{l} - 2m \right) D_m^N \right] \\ + K_N \left[ \sum_{m=0}^{\lfloor N/2 \rfloor} \sum_{n=2}^{N-2m-1} (-1)^{m+1} \frac{(N-m-n)!(n-2)!}{N!} E_{m,n}^N \right] - \ln K_N. \quad (4.22)$$

This expression is given in terms of various symmetric functions of the squares of the chordal distances, namely

$$D_m^N = \sum_{i_1=1}^N \sum_{j_1>i_1}^N \sum_{i_2>i_1}^N \sum_{j_2>i_2}^N \dots \sum_{i_m>i_{m-1}}^N \sum_{j_m>i_m}^N \sigma_{i_1 j_1} \sigma_{i_2 j_2} \dots \sigma_{i_m j_m} \\ E_{m,n}^N = \sum_{i_1=1}^N \sum_{j_1=1}^N \sum_{j_2>j_1}^N \dots \sum_{j_n>j_{n-1}}^N \sum_{k_1=1}^N \sum_{l_1>k_1}^N \sum_{k_2>k_1}^N \sum_{l_2>k_2}^N \dots \\ \sum_{k_m>k_{m-1}}^N \sum_{l_m>k_m}^N \sigma_{i_j} \sigma_{i_j} \dots \sigma_{i_j} \sigma_{k_1 l_1} \sigma_{k_2 l_2} \dots \sigma_{k_m l_m}.$$

and

$$K_N^{-1} = \sum_{m=0}^{\lfloor N/2 \rfloor} (-1)^m \frac{(N-m)!}{N!} D_m^N \quad \text{where} \quad \lfloor N/2 \rfloor = \begin{cases} N/2 & \text{if } N \text{ is even} \\ \frac{N-1}{2} & \text{if } N \text{ is odd.} \end{cases}$$

We thus have an expression for  $S_W$  which we can maximize with respect to  $\theta_i$  and  $\phi_i$ . The configurations for which the Wehrl entropy is maximized are shown (albeit somewhat rotated) in Tables 4.1 and 4.2.

The second derivative test is a useful criterion for determining whether a given critical point of a function of one variable is a local maximum or not. It states that if the first derivative of the function is zero at a critical point  $x$ , and if the second derivative less than zero at  $x$ ,  $x$  is a local maximum. For a function of more than one variable, the second-derivative test generalizes to a test based on the eigenvalues of the function's Hessian matrix at the critical point. If the eigenvalues of the Hessian at the critical point are all negative, then the critical point is a local maximum. Hence we study the eigenvalues of the Hessian of  $S_W$ , with the first derivatives  $\Delta\theta$  and  $\Delta\phi$  equal to zero. All eigenvalues are negative for the optimal arrangements given in Tables 4.1 and 4.2, which shows that the corresponding Wehrl entropy is (at least locally) maximized.

<sup>1</sup>Eq. (3.19) in Ref. [16] contains a misprint

#### 4.4 Optimal Arrangements

Recall that a general pure state can be written in the form (2.9), where we use  $|e_k\rangle = \{|j, m\rangle\}$  as our set of orthonormal basis vectors for the Hilbert space and  $n = 2j$ . We now consider a state that is represented by  $j + m_2$  points where  $\mathbf{n}$  meets the sphere,  $j + m_1$  points at the antipode and a band of  $\Delta m = m_1 - m_2$  points around the sphere at some angle  $\theta$ . Without loss of generality we can assume that this corresponds to  $j + m_2$  points at the North pole and  $j + m_1$  points at the South pole. We also assume that there are  $\Delta m = m_1 - m_2$  points around the equator. Note that for constant latitude, the band of  $\Delta m$  points make up vertices in a regular polygon.

The corresponding polynomial is given by

$$w(z) = z^{j+m_1} - z^{j+m_2} \left( \tan \frac{\theta}{2} e^{i\phi} \right)^{\Delta m}. \quad (4.23)$$

Since (4.23) must equal the polynomial (2.16),

$$\sum_{k=0}^{2j} (-1)^k Z_k \sqrt{\binom{2j}{k}} z^{2j-k} = z^{j+m_1} - \left( \tan \frac{\theta}{2} e^{i\phi} \right)^{\Delta m} z^{j+m_2},$$

we find that the only nonzero coordinates are the terms for which the exponents are equal, that is  $2j - k = j + m_1$  and  $2j - k = j + m_2$ . Thus the only non-zero coordinates are

$$Z_{j-m_1} = \frac{(-1)^{j-m_1}}{\sqrt{\binom{2j}{j-m_1}}} \quad \text{and} \quad Z_{j-m_2} = \frac{(-1)^{j-m_2+1} \left( \tan \frac{\theta}{2} e^{i\phi} \right)^{\Delta m}}{\sqrt{\binom{2j}{j-m_2}}},$$

and the state is then given by

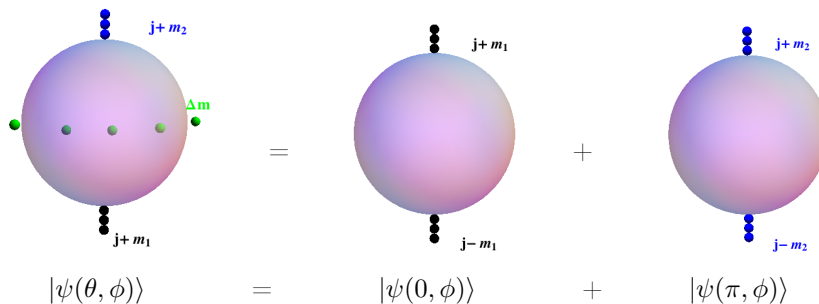
$$|\psi\rangle = \sum_{k=0}^{2j} Z_k |j, m\rangle = Z_{j-m_1} |j, m_1\rangle + Z_{j-m_2} |j, m_2\rangle. \quad (4.24)$$

The state does not change when multiplying with a constant factor. Hence we can simplify (4.24) by multiplying it with  $(-1)^{j+m_1} \sqrt{(2j)!}$  and thereby obtain the following expression for the state in terms of  $\theta$  and  $\phi$

$$\begin{aligned} |\psi(\theta, \phi)\rangle &= \sqrt{(j+m_1)!(j-m_1)!} |j, m_1\rangle \\ &+ (-1)^{\Delta m+1} \sqrt{(j+m_2)!(j-m_2)!} \left( \tan \frac{\theta}{2} e^{i\phi} \right)^{\Delta m} |j, m_2\rangle. \end{aligned} \quad (4.25)$$

Since the system is rotationally invariant (the Wehrl entropy does not change for a rotation by an angle  $\phi$  around the  $z$ -axis), the state only depends on the angle  $\theta$ .

Figure 4.2: The state which corresponds to  $j + m_2$  points at  $\theta = 0$ ,  $j + m_1$  points at  $\theta_1 = \pi$  and  $\Delta m = m_1 - m_2$  points at  $\theta_2 = \pi/2$  interpolates between the state  $|\psi(0, \phi)\rangle$  and the state  $|\psi(\pi, \phi)\rangle$ .



In Fig. 4.2 we see how the state  $|\psi(\theta, \phi)\rangle$  is composed of the two states  $|\psi(0, \phi)\rangle$  and  $|\psi(\pi, \phi)\rangle$ . This system corresponds to a rotation-invariant two-dimensional subspace. The polynomial describing the state  $|\psi(0, \phi)\rangle$  is given by  $w(z) = z^{j+m_1}$ , which yields the following expression for  $|\psi(0, \phi)\rangle$

$$\begin{aligned} |\psi(0, \phi)\rangle &= Z_{j-m_1} |j, m_1\rangle \\ &= \frac{(-1)^{j-m_1}}{\sqrt{\binom{2j}{j-m_1}}} |j, m_1\rangle, \end{aligned}$$

with  $j + m_1$  points at the North pole and  $j - m_1$  at the South pole. The other state is defined for  $\theta = \pi$  in a similar way but with  $j + m_2$  points at the North pole and  $j - m_2$  at the South pole.

## 4.5 Results

In this section we present the results of our investigation of spherical arrangements of 2-9 points on the unit sphere which maximize the Wehrl entropy  $S_W$ . We define the optimal configurations as the arrangements which yield maximal  $S_W$  and thus correspond to the most non-coherent states. To find these, we consider configurations that solve the Thomson problem, the Toth problem and the QQ problem and investigate whether they give local maxima to the Wehrl entropy. The optimal spherical arrangements for the four problems (Thomson, Toth, QQ and Wehrl) are shown in Tables 4.1 and 4.2 together with the resulting Wehrl entropy. We find that the configurations that solve the four problems are equal up to 6 points.

- $n = 1$ : In this case all pure states are coherent, and hence the minimal Wehrl entropy equals the maximal Wehrl entropy, that is  $S_{\min} = S_{\max} = 1/2$ . This is the trivial case.

- $n = 2$ : For two points the optimal arrangements for the Thomson, Toth and QQ problems agree, and this optimal configuration is given by two points diametrically opposite to each other. This is quite intuitive; if we want to place two points on a sphere as far from each other as possible, we place them antipodally. The maximal Wehrl entropy is  $S_W = 0.973519$ , which in this case is a global maximum.
- $n = 3$ : For three points the optimal arrangements for the Thomson, Toth and QQ problems agree, and give a local maximum for the Wehrl entropy. The optimal configuration is given by three points forming an equilateral triangle on a large circle. This follows our hypothesis that the further away points are from each other, the larger the Wehrl entropy becomes. The maximal Wehrl entropy is  $S_W = 1.23871$ .
- $n = 4$ : For four points the optimal arrangements for the Thomson, Toth and QQ problems agree, and give a local maximum for the Wehrl entropy. The optimal configuration is a regular polyhedra, namely a tetrahedron. The maximal Wehrl entropy is  $S_W = 1.49166$ .
- $n = 5$ : For five points there are two arrangements that are likely to give local maxima for the Wehrl entropy. A configuration for which a local maximum of the Wehrl entropy indeed occurs is given by three equidistant points on the equator together with two points at the poles. This arrangement is optimal also for the Thomson, Toth and QQ problems. The maximal Wehrl entropy is  $S_W = 1.65531$ .

The second interesting configuration that we consider is given by an octahedron minus a single point. This arrangement is one of two solutions to the Toth problem, since the minimum pairwise distance between all pair of points in this configuration is equal to that given by the configuration consisting of three equidistant points on the equator and two points at the poles. The Wehrl entropy for a configuration consisting of a octahedron minus a single point is  $S_W = 1.65163$ , which is somewhat lower than the maximal value  $S_W = 1.65531$ . This configuration does not correspond to a local maximum, since not all eigenvalues are negative.

- $n = 6$ : For six points the optimal arrangements for the Thomson, Toth and QQ problems agree, and give a local maximum for the Wehrl entropy. The optimal configuration is once again a regular polyhedron, namely the octahedron. The maximal Wehrl entropy is  $S_W = 1.83594$ .
- $n = 7$ : For seven points the optimal arrangements for the four problems differ for the first time. The configuration that solves the Thomson problem, the QQ problem and for which a local maximum of the Wehrl entropy occurs is a pentagonal dipyramid, where five points lie on an equatorial pentagon and the other two on the poles. The maximal Wehrl entropy  $S_W = 1.95286$ .

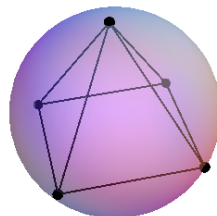


Figure 4.3:  $S_W = 1.65163$  for the configuration given by the octahedron minus a single point. This is less than the maximal Wehrl entropy  $S_W = 1.65531$ .

However, the configuration that solves the Toth problem consists of two triangles asymmetrically positioned about the equator with the remaining point at a pole. The Wehrl entropy of such a configuration is  $S_W = 1.94987$ , which is lower than the maximal  $S_W$ . This configuration does not correspond to a local maximum, since not all eigenvalues are negative.

- $n = 8$ : Since there exists a platonic solid for eight points, our first approach is to investigate whether the cube gives a maximal Wehrl entropy of  $S_W = 2.06683$ . However, this configuration is not a local maximum. Instead the arrangement for which a local maximum of the Wehrl entropy occur is that of a cubic antiprism, which can be obtained from a cube by rotating one face by 45 degrees. The distances between neighboring vertices are the same, and the maximal Wehrl entropy is  $S_W = 2.07789$ .

The Thomson problem and the Toth problem are also solved by a cubic antiprism, but for slightly different values of the polar angle  $\theta$  from the North pole to the upper and lower faces, which results in lower values of  $S_W$ .

The solution to the QQ problem is completely different compared to the other solutions, as the configuration in this case consists of two irregular rectangles perpendicular to each other. Such a configuration results in a Wehrl entropy of  $S_W = 2.07535$ , and does not correspond to a local maximum.

- $n = 9$ : For nine points the optimal configuration is a triaugmented triangular prism state consisting of three equilateral triangles that are positioned parallel but asymmetric to each other. This gives a local maximum for the Wehrl entropy. The maximal Wehrl entropy is  $S_W = 2.18494$ .

The Thomson problem, the Toth problem and the QQ problem are also solved by this configuration, but with slightly different values of the polar angle  $\theta$  from the North pole to the triangles, which once again results in lower values of  $S_W$ .

We have now achieved our main goal, which was to maximize the Wehrl entropy in finite dimensions. To this end we considered spherical arrangements of points.



We found local maxima for the Wehrl entropy for 2-9 points, and presented our results in Tables 4.1 and 4.2.

The next step is to study part of the proof of the Lieb conjecture in order to give a geometric illustration of how quantum channels for coherent states majorize all other quantum channels. This will be further described in the next section.





















	Optimal Configuration	QQ	Thomson	Toth	No. of points
$S_W$					$n = 2$
$S_W$	0.973519	0.973519	0.973519	0.973519	
					$n = 3$
$S_W$	1.23871	1.23871	1.23871	1.23871	
					$n = 4$
$S_W$	1.49166	1.49166	1.49166	1.49166	
					$n = 5$
$S_W$	1.65531	1.65531	1.65531	1.65531	
					$n = 6$
$S_W$	1.83594	1.83594	1.83594	1.83594	

Table 4.1: Arrangements of points on a Bloch sphere that give maximal Wehrl entropy, where  $n$  is the number of points for dimension  $N = n + 1$  and  $S_W$  is the Wehrl entropy. For  $n = 2-6$  points, the optimal configurations are equal for the Thomson problem, Toth problem, QQ article and Wehrl maximization. The only exception is for the Toth problem, which is also solved by the arrangement shown in Fig. 4.3.

	Optimal Configuration	QQ	Thomson	Toth	No. of points
$S_W$	1.95286	1.95286	1.95286	<u>&lt;1.95286</u>	$n = 7$
$S_W$	2.07789	<u>2.07535</u>	<u>&lt; 2.07789</u>	<u>&lt; 2.07789</u>	$n = 8$
$S_W$	2.18494	<u>2.18479</u>	<u>&lt;2.18494</u>	<u>&lt;2.18494</u>	$n = 9$

Table 4.2: Arrangements of points on a Bloch sphere that give maximal Wehrl entropy, where  $n$  is the number of points for dimension  $N = n + 1$  and  $S_W$  is the Wehrl entropy. For  $n = 7$ ,  $n = 8$  and  $n = 9$  points the optimal configurations for the Toth problem and the QQ problem differ from optimal configuration, which results in a lower value of  $S_W$ . The configurations resulting in non-optimal values of  $S_W$  are underlined.

Figure 4.4: Illustration of how the Wehrl entropy for the optimal configurations shown in Table 4.1 depends on the parameter  $\theta$  (with fixed  $\phi$ ) for  $n = 2-5$  points on the unit sphere.

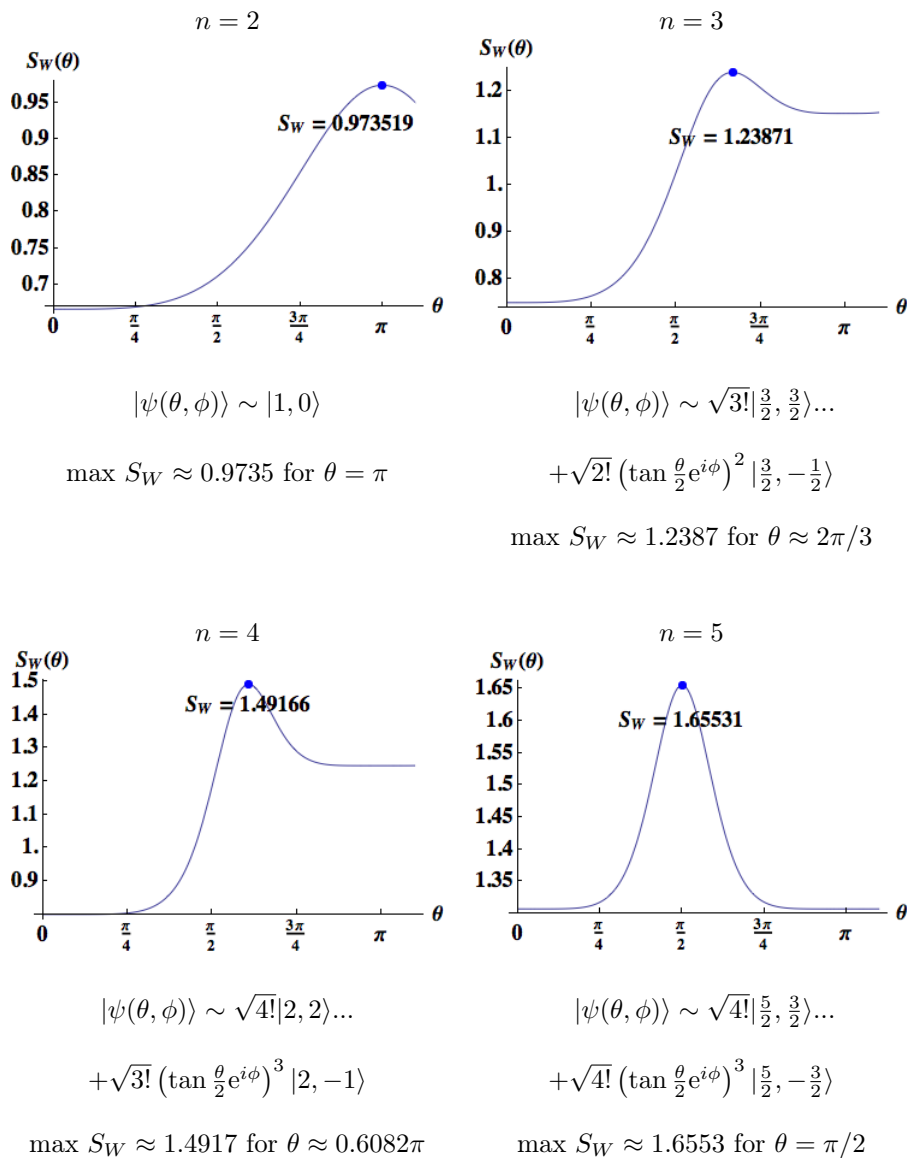


Figure 4.5: Illustration of how the Wehrl entropy for the optimal configurations shown in Table 4.2 depends on the parameter  $\theta$  (with fixed  $\phi$ ) for  $n = 6$  and  $n = 7$  points on the unit sphere.

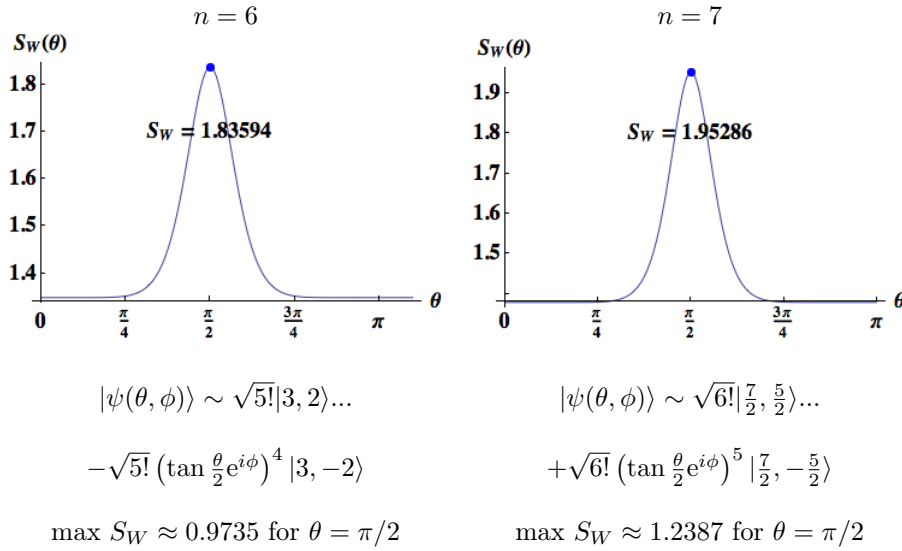
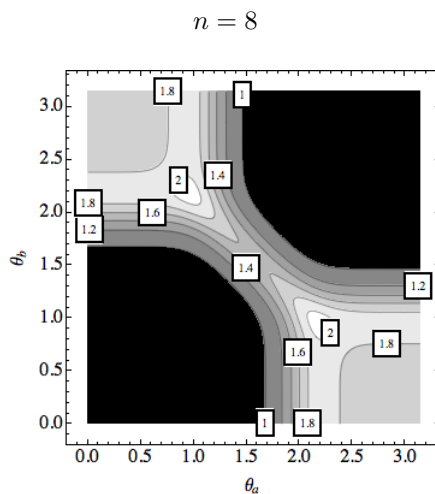


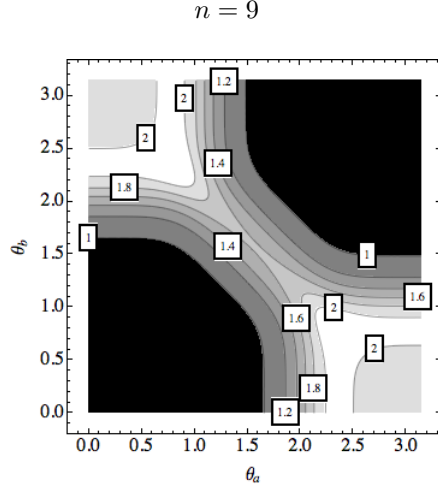
Figure 4.6: Illustration of how the Wehrl entropy for the optimal configurations shown in Table 4.2 depends on the parameter  $\theta$  (with fixed  $\phi$ ) for  $n = 8$  points on the unit sphere. Note that the optimal configurations depend on two  $\theta$ , resulting in a contour plot.



$$\begin{aligned}
 |\psi(\theta, \phi)\rangle &\sim \sqrt{8!}|4, 4\rangle - \sqrt{4!8!} \left(\tan \frac{\theta_2}{2} e^{i\phi_2}\right)^4 |4, 0\rangle \dots \\
 &\quad - \sqrt{4!8!} \left(\tan \frac{\theta_1}{2} e^{i\phi_1}\right)^4 |4, 0\rangle \dots \\
 &\quad + \sqrt{8!} \left(\tan \frac{\theta_1}{2} \tan \frac{\theta_2}{2} e^{i(\phi_1+\phi_2)}\right)^8 |4, -4\rangle
 \end{aligned}$$

$$\max S_W \approx 2.07789 \text{ for } \theta_a \approx 0.3045\pi, \theta_b \approx 0.6955\pi$$

Figure 4.7: Illustration of how the Wehrl entropy for the optimal configurations shown in Table 4.2 depends on the parameter  $\theta$  (with fixed  $\phi$ ) for  $n = 9$  points on the unit sphere. Note that the optimal configurations depend on two  $\theta$ , resulting in a contour plot.



$$\begin{aligned}
|\psi(\theta, \phi)\rangle &\sim \sqrt{9!} \left| \frac{9}{2}, \frac{9}{2} \right\rangle - \sqrt{3!6!} (\tan \frac{\theta_3}{2} e^{i\phi_3})^3 \left| \frac{9}{2}, \frac{3}{2} \right\rangle \dots \\
&\quad - \sqrt{3!6!} (\tan \frac{\theta_2}{2} e^{i\phi_2})^3 \left| \frac{9}{2}, \frac{3}{2} \right\rangle - \sqrt{3!6!} (\tan \frac{\theta_1}{2} e^{i\phi_1})^3 \left| \frac{9}{2}, \frac{3}{2} \right\rangle \dots \\
&\quad - \sqrt{3!6!} (\tan \frac{\theta_2}{2} \tan \frac{\theta_3}{2} e^{i(\phi_2+\phi_3)})^3 \left| \frac{9}{2}, -\frac{3}{2} \right\rangle \dots \\
&\quad - \sqrt{3!6!} (\tan \frac{\theta_1}{2} \tan \frac{\theta_3}{2} e^{i(\phi_1+\phi_3)})^3 \left| \frac{9}{2}, -\frac{3}{2} \right\rangle \dots \\
&\quad - \sqrt{3!6!} (\tan \frac{\theta_1}{2} \tan \frac{\theta_2}{2} e^{i(\phi_1+\phi_2)})^3 \left| \frac{9}{2}, -\frac{3}{2} \right\rangle \dots \\
&\quad - \sqrt{9!} (\tan \frac{\theta_1}{2} \tan \frac{\theta_2}{2} \tan \frac{\theta_3}{2} e^{i(\phi_1+\phi_2+\phi_3)})^3 \left| \frac{9}{2}, -\frac{9}{2} \right\rangle
\end{aligned}$$

$$\max S_W \approx 2.18494 \text{ for } \theta_a \approx 0.2529\pi, \theta_b \approx 0.7471\pi$$

## 4.6 Comment on the Proof of the Lieb Conjecture

In this section we use results from Ref. [25] in order to give a geometric illustration of how quantum channels for coherent states majorize all other quantum channels. This is the key point in the proof of the Lieb conjecture by Lieb and Solovej. We do not present the whole proof here.

Consider a density matrix  $\rho = |\psi\rangle\langle\psi|$  on  $\mathcal{H}$ , where  $\rho$  is a positive semi-definite operator with trace  $\text{Tr}[\rho] = 1$ . According to Lieb, the Wehrl entropy is minimized when  $\rho$  is a one-dimensional projection onto any coherent state  $|p, q\rangle$ , i.e.  $\rho = |p, q\rangle\langle p, q|$ . We recall that the Wehrl entropy is defined as a concave function of the Husimi function, namely  $S_W(\rho) \sim -\int d\Omega Q \ln Q$ , and that Lieb proved that the minimum classical entropy for canonical coherent states occurs for density matrices equal to projectors onto coherent states (Section 4.2). This is true also for Bloch  $SU(2)$  spin-coherent states for every angular momentum  $J$ , i.e. the classical entropy is minimized by Bloch coherent states. The proof holds for all concave functions  $f(t)$ , not just those of the form  $f(t) = -t \ln(t)$ , and utilizes coherent operators. These are operators that map density matrices in an  $SU(2)$  space characterized by an angular momentum  $m+1$ , to a density matrix in a spin  $n+1$  space. Such maps are given by  $\Phi^{m-n}(\rho)$ , which is defined below.

Lieb and Solovej prove in [25] that for every finite  $m+1$ , the projections onto coherent states in a spin  $n+1$  space minimize the von Neumann entropy of the density matrix in a spin  $m+1$  space. We show this for the map  $\Phi^2(\rho)$  in a geometric illustration.

### $\Phi^{m-n}(\rho)$ in the Schwinger Representation

The map  $\Phi^{m-n}(\rho)$  has a simple form using the creation and annihilation operators introduced by Schwinger [35]. Let  $\mathcal{H}_J$  denote the spin  $J$  representation space of  $SU(2)$  for all integer or half-integer  $J$ . The corresponding classical phase space is  $\mathbf{S}^2$ . For each point  $\omega$  in  $\mathbf{S}^2$  there is a one-dimensional coherent state projection  $P_\omega^J = |\omega\rangle_{JJ}\langle\omega|$  projecting  $\mathcal{H}_J$  onto the subspace of maximal spin in the direction  $\omega$ . This one-dimensional subspace of  $\mathcal{H}_J$  is the eigenspace of  $\omega \cdot \mathbf{S}_J$  with eigenvalue  $J$ . Note that  $\mathbf{S}_J$  is the representation on  $\mathcal{H}_J$  of the standard generators  $\mathbf{S} = (S_x, S_y, S_z)$  of  $SU(2)$ . The operators

$$\begin{aligned} S_x &= \frac{1}{2}(a_\uparrow^* a_\downarrow + a_\downarrow^* a_\uparrow) \\ S_y &= \frac{1}{2i}(a_\uparrow^* a_\downarrow - a_\downarrow^* a_\uparrow) \\ S_z &= \frac{1}{2}(a_\uparrow^* a_\uparrow - a_\downarrow^* a_\downarrow) \end{aligned}$$

satisfy the correct commutation relations and  $S_x^2 + S_y^2 + S_z^2 = J(J+1)$ . We also have the relation  $a_\uparrow^* a_\uparrow + a_\downarrow^* a_\downarrow = 2J$ , where the annihilation operators  $a_\uparrow$  and  $a_\downarrow$  are the adjoints of  $a_\uparrow^*$  and  $a_\downarrow^*$ .



The Hilbert space  $\mathcal{H}_J$  may be identified with the completely symmetric subspace  $\otimes_{\text{sym}}^{2J} \mathcal{H}_{1/2}$  of the tensor product  $\otimes^{2J} \mathcal{H}_{1/2}$ . Here  $\mathcal{H}_{1/2}$  is the one-particle space and  $a_{\uparrow}^*$  and  $a_{\downarrow}^*$  the creation operators corresponding to spin up and down respectively. These operators map  $\otimes_{\text{sym}}^l \mathcal{H}_{1/2}$  to  $\otimes_{\text{sym}}^{l+1} \mathcal{H}_{1/2}$  for all positive integers  $l$ . Then, for  $\psi \in \otimes_{\text{sym}}^l \mathcal{H}_{1/2}$  and with  $P_{\text{sym}}$  as the projection onto the symmetric space  $\otimes_{\text{sym}}^{l+1} \mathcal{H}_{1/2}$ , we have

$$a_{\uparrow}^* \psi = \sqrt{l+1} P_{\text{sym}}(|\uparrow\rangle_{\frac{1}{2}} \otimes \psi) \quad (4.26)$$

and likewise for  $a_{\downarrow}^*$ .

The symmetric subspace of  $\otimes^{2J} \mathcal{H}_{1/2}$  is the subspace corresponding to  $2J$  bosonic particles. We can then identify the spin representation on the Hilbert space  $\mathcal{H}_J$  with the space of  $2J$  bosons over a two-dimensional one-particle space. In particular,  $a_{\omega}^*$  is the creation of a particle in the state  $|\omega\rangle_{\frac{1}{2}}$ , i.e.  $a_{\omega}^* = \langle \uparrow | \omega \rangle_{\frac{1}{2}} a_{\uparrow}^* + \langle \downarrow | \omega \rangle_{\frac{1}{2}} a_{\downarrow}^*$ , where  $|0\rangle$  is the vacuum state and  $|\omega\rangle_J \in \mathcal{H}_J$  is a coherent state. Using the canonical commutation relations, we see that all creation operators commute and that  $[a_{\omega}^*, a_{\omega}^*] = \frac{1}{2} \langle \omega' | \omega \rangle_{\frac{1}{2}}$ , which gives us the relation

$$a_{\uparrow} a_{\uparrow}^* + a_{\downarrow} a_{\downarrow}^* = a_{\uparrow}^* a_{\uparrow} + a_{\downarrow}^* a_{\downarrow} + 2 = 2J + 2. \quad (4.27)$$

If  $\rho$  is a non-negative density matrix on  $\mathcal{H}_{n/2}$ , meaning that its eigenvalues are positive, then the map of  $\rho$  is also non-negative and can be defined as

$$\Phi^{m-n}(\rho) = \frac{(n+1)!}{(m+1)!} \sum_{i_1, \dots, i_k = \uparrow, \downarrow} a_{i_k} \dots a_{i_1} \rho a_{i_1}^* \dots a_{i_k}^* \quad (4.28)$$

in terms of creation and annihilation operators.

This map is trace-preserving. To show this we first consider the case

$$\text{Tr}[\Phi^1(\rho)] = \frac{1}{n+2} \text{Tr}[a_{\uparrow}^* \rho a_{\uparrow} + a_{\downarrow}^* \rho a_{\downarrow}].$$

Using the relation  $\text{Tr}[ABC] = \text{Tr}[CAB]$  and the commutation relation  $[a_{\uparrow}, a_{\uparrow}^*] = a_{\uparrow} a_{\uparrow}^* - a_{\uparrow}^* a_{\uparrow} = 1$ , we obtain

$$\text{Tr}[\Phi^1(\rho)] = \frac{1}{n+2} \text{Tr}[(a_{\uparrow} a_{\uparrow}^* - a_{\uparrow}^* a_{\uparrow} + 2)\rho] = \frac{1}{n+2} \text{Tr}[(n+2)\rho] = \text{Tr}[\rho].$$

Since  $\text{Tr}[\rho] = 1$  we have  $\text{Tr}[\Phi^1(\rho)] = 1$ . Using the fact that  $\Phi^2(\rho) = \Phi^1(\Phi^1(\rho))$ , we see that all  $\Phi^{m-n}(\rho)$  are trace-preserving. In the language of quantum information theory, this trace-preserving map is a quantum channel.

## Geometric Illustration of Quantum States

We illustrate that the map of the density matrix of coherent states majorizes  $\Phi^{m-n}(\rho)$  for all other density matrices, i.e. that  $\Phi^{m-n}(|n, 0\rangle\langle n, 0|) \succ \Phi^{m-n}(\rho)$  for all  $\rho$ . This is done by studying the spectrums of  $\Phi^{m-n}(|n, 0\rangle\langle n, 0|)$  and  $\Phi^{m-n}(\rho)$ .

Consider two positive vectors  $\vec{a}$  and  $\vec{b}$  with components ordered in decreasing order,  $a_1 \geq a_2 \geq \dots \geq a_M$ . The finite real sequence  $b_1 \geq b_2 \geq \dots \geq b_M$  is majorized by another real sequence  $a_1 \geq a_2 \geq \dots \geq a_M$ , written  $a_1 \geq a_2 \geq \dots \geq a_M \succ b_1 \geq b_2 \geq \dots \geq b_M$  or  $\vec{a} \succ \vec{b}$ , if

$$\begin{aligned} a_1 &\geq b_1 \\ a_1 + a_2 &\geq b_1 + b_2 \\ &\dots \\ a_1 + \dots + a_{M-1} &\geq b_1 + \dots + b_{M-1} \\ a_1 + \dots + a_M &= b_1 + \dots + b_M. \end{aligned} \tag{4.29}$$

We consider density matrices  $\rho = |\psi\rangle\langle\psi|$  defined for state vectors of the form  $|\psi\rangle = \cos\frac{\theta}{2}|n, 0\rangle + \sin\frac{\theta}{2}e^{i\phi}|1, n-1\rangle$ . Note that this state vector is a superposition of a coherent state  $|n, 0\rangle$  and a general state  $|1, n-1\rangle$ . The spectrum for  $\Phi^2(\rho)$  is calculated for 2-5 qubits and graphically presented in Fig. 4.8. The non-trivial spectrum of  $\Phi^2(\rho)$  consists of a three-dimensional vector  $[p_1, p_2, p_3]$  where  $\sum p_i = 1$ . This corresponds to a point in a triangle whose vertices are given by the vectors  $[1, 0, 0]$ ,  $[0, 1, 0]$  and  $[0, 0, 1]$ . The spectrum for a coherent state  $|\psi\rangle = |n, 0\rangle$  with  $\theta = 0$  is represented by a point in the aforementioned triangle. By mirroring this point in all medians, we obtain a polygon inside the triangle.

Our assumption is that  $\Phi^2(|n, 0\rangle\langle n, 0|) \succ \Phi^2(\rho)$ . If this assumption is true, the points representing all other spectra must be included inside the polygon. Thus, in order to prove  $\Phi^2(|n, 0\rangle\langle n, 0|) \succ \Phi^2(\rho)$ , we have to calculate the eigenvalues for arbitrary  $\theta$ ,  $0 \leq \theta < \pi$ , to see whether they end up inside the polygon.

In Fig. 4.8, we show that this is true for 2-5 points. This gives a geometric illustration of  $\Phi^2(|n, 0\rangle\langle n, 0|) \succ \Phi^2(\rho)$ . Furthermore, this corresponds to a geometrical comparison of the spectra of the Wehrl entropy and the von Neumann entropy. We show that the most non-coherent states, which correspond to maximal Wehrl entropy, also give maximal von Neumann entropy. Analogously, the coherent states that give minimum Wehrl entropy also minimize the von Neumann entropy.

Explanations of the geometric illustration of the spectrums are listed below.

- $n = 2$ : The spectrum for the coherent state  $|\psi\rangle = |2, 0\rangle$  is given by the vector  $[3/10, 4/10, 3/10]$ , which corresponds to the large blue point on the left side. By mirroring this point in all medians, we obtain the polygon with blue vertices. The spectra for all states  $|\psi\rangle = \cos\frac{\theta}{2}|2, 0\rangle + \sin\frac{\theta}{2}e^{i\phi}|1, 1\rangle$  are given by the black line in the figure. Since this is inside the polygon for all  $\theta$ , with the largest value being the aforementioned coherent state, we have that  $\Phi^2(|2, 0\rangle\langle 2, 0|)$  majorizes  $\Phi^2(\rho)$ .

The maximal von Neumann entropy  $S = \max(-\sum_i p_i \lg[p_i]) = 1.0889$  for  $\theta = \pi$  corresponds to the green point and is given by the eigenvalue-vector closest to the midpoint  $[1/3, 1/3, 1/3]$ , which corresponds to the black point. The maximal Wehrl entropy  $S_W = 0.974$  is given by  $\theta = \pi$ , which corresponds

to the pink point. Note that the maximal Wehrl entropy is given by the same state vector as the one which yields maximal von Neumann entropy. Thus the maximal von Neumann entropy is given by the most non-coherent state, which also yields maximal Wehrl entropy.

The minimal von Neumann entropy  $S = \min(-\sum_i p_i \lg[p_i]) = 0.8979$  is given by  $\theta = 0$ , which corresponds to the coherent state  $|\psi\rangle = |2, 0\rangle$ . Thus the minimal von Neumann entropy is given by a coherent state, which also yields minimal Wehrl entropy.

- $n = 3$ : The spectrum for the coherent state  $|\psi\rangle = |3, 0\rangle$  is given by the vector  $[4/15, 1/15, 2/3]$ , which corresponds to the large blue point on the left side. The spectra for all states  $|\psi\rangle = \cos \frac{\theta}{2} |3, 0\rangle + \sin \frac{\theta}{2} e^{i\phi} |1, 2\rangle$  are given by the black line in the figure. Since this is inside the polygon for all  $\theta$ , with the largest value being the aforementioned coherent state, we have that  $\Phi^2(|3, 0\rangle\langle 3, 0|) \succ \Phi^2(\rho)$ .

The maximal von Neumann entropy  $S = 1.0882$  and the maximal Wehrl entropy  $S_W = 1.239$  are both given by  $\theta \approx 2\pi/3$ , which corresponds to the green point and pink point respectively. Since the maximal Wehrl entropy is given by the same state vector as the one which yields maximal von Neumann entropy, they are represented by the same point in the triangle. Thus the maximal von Neumann entropy is given by the most non-coherent state, which also yields maximal Wehrl entropy.

The minimal von Neumann entropy  $S = 0.8033$  is given by  $\theta = 0$ , which corresponds to the coherent state  $|\psi\rangle = |3, 0\rangle$ . Thus the minimal von Neumann entropy is given by a coherent state, which also yields minimal Wehrl entropy.

- $n = 4$ : The spectrum for the coherent state  $|\psi\rangle = |4, 0\rangle$  is given by the vector  $[1/21, 5/21, 5/7]$ , which corresponds to the large blue point on the left side. The spectra for all states  $|\psi\rangle = \cos \frac{\theta}{2} |4, 0\rangle + \sin \frac{\theta}{2} e^{i\phi} |1, 3\rangle$  are given by the black line in the figure. Since this is inside the polygon for all  $\theta$ , with the largest value being the aforementioned coherent state, we have that  $\Phi^2(|4, 0\rangle\langle 4, 0|) \succ \Phi^2(\rho)$ .

The maximal von Neumann entropy  $S = 1.09861$  and the maximal Wehrl entropy  $S_W = 1.492$  are both given by  $\theta \approx 0.608\pi$ , which corresponds to the green point and pink point respectively. Since the maximal Wehrl entropy is given by the same state vector as the one which yields maximal von Neumann entropy, they are represented by the same point in the triangle. Thus the maximal von Neumann entropy is given by the most non-coherent state, which also yields maximal Wehrl entropy.

The minimal von Neumann entropy  $S = 0.7270$  is given by  $\theta = 0$ , which corresponds to the coherent state  $|\psi\rangle = |4, 0\rangle$ . Thus the minimal von Neumann entropy is given by a coherent state, which also yields minimal Wehrl entropy.

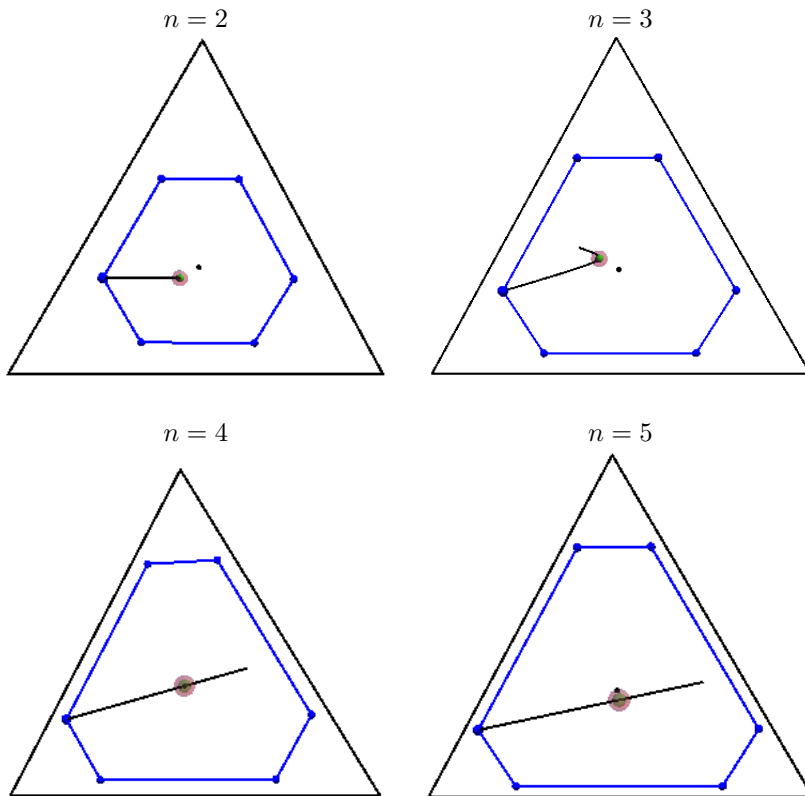
- $n = 5$ : The spectrum for the coherent state  $|\psi\rangle = |5, 0\rangle$  is given by the vector  $[1/28, 3/14, 3/4]$ , which corresponds to the large blue point on the left side. The spectra for all states  $|\psi\rangle = \cos \frac{\theta}{2} |5, 0\rangle + \sin \frac{\theta}{2} e^{i\phi} |1, 4\rangle$  are given by the black line in the figure. Since this is inside the polygon for all  $\theta$ , with the largest value being the aforementioned coherent state, we have that  $\Phi^2(|5, 0\rangle\langle 5, 0|) \succ \Phi^2(\rho)$ .

The maximal von Neumann entropy  $S = 1.0967$  and the maximal Wehrl entropy  $S_W = 1.655$  are both given by  $\theta = \frac{\pi}{2}$ , which corresponds to the green point and pink point respectively. Since the maximal Wehrl entropy is given by the same state vector as the one which yields maximal von Neumann entropy, they are represented by the same point in the triangle. Thus the maximal von Neumann entropy is given by the most non-coherent state, which also yields maximal Wehrl entropy.

The minimal von Neumann entropy  $S = 0.6649$  is given by  $\theta = 0$ , which corresponds to the coherent state  $|\psi\rangle = |5, 0\rangle$ . Thus the minimal von Neumann entropy is given by a coherent state, which also yields minimal Wehrl entropy.

We have thereby showed that  $\Phi^2(|n, 0\rangle\langle n, 0|) \succ \Phi^2(\rho)$ , i.e. that the map of coherent states majorizes the map of all other states. Furthermore we have showed that the most non-coherent states which correspond to maximal Wehrl entropy, also give maximal von Neumann entropy, and that the coherent states that give minimum Wehrl entropy also minimize the von Neumann entropy.

Figure 4.8: Geometric illustration of the spectrum of the map  $\Phi^2(\rho)$  for  $n = 2-5$  points on a sphere, for  $\rho = |\psi\rangle\langle\psi|$  and  $|\psi\rangle = \cos\frac{\theta}{2}|n, 0\rangle + \sin\frac{\theta}{2}e^{i\phi}|1, n-1\rangle$ .





## Chapter 5

# Geometric Entanglement of Symmetric States

In this chapter we present a geometrical interpretation of the entanglement of permutation-symmetric states in the form of the Majorana representation. By means of this representation we see how symmetry allows us to calculate the geometric measure of entanglement and identify the most entangled state. The calculation of the maximal geometric measure of entanglement is phrased as a geometric optimization problem. We explore the maximally entangled symmetric states of 2-9 qubits and their amount of geometric entanglement following Ref. [38]. We then use these results to investigate how the maximally entangled symmetric states are related to the states corresponding to maximal Wehrl entropy.

We start by considering the symmetric basis states, known as the Dicke states, of a system of  $n$  qubits in the symmetric Hilbert space  $\mathcal{H}_N$ . A Dicke state is the sum of all permutations of computational basis states with  $n - k$  qubits being  $|0\rangle$  and  $k$  being  $|1\rangle$

$$|S_{n,k}\rangle = \binom{n}{k}^{-1/2} \sum_{\text{perm}} \underbrace{|0\rangle \dots |0\rangle}_{n-k} \underbrace{|1\rangle \dots |1\rangle}_k \quad (5.1)$$

with  $0 \leq k \leq n$ . This corresponds to  $n - k$  points at the North pole ( $\theta = 0$ ) and  $k$  points at the South pole ( $\theta = \pi$ ) on the Bloch sphere. A general pure symmetric state of  $n$  qubits is a linear combination of the  $n + 1$  symmetric basis states  $|S_{n,k}\rangle$ . We abbreviate this notation to  $|S_k\rangle$  when the number of qubits is clear.

In the Dicke state representation, any symmetric state  $|\psi\rangle_S$  is expanded in the orthonormal basis formed by the  $n + 1$  Dicke states in the symmetric subspace  $\mathbb{C}^N$ :

$$|\psi\rangle_S = \sum_{k=0}^n a_k |S_k\rangle, \quad (5.2)$$

where  $a_k$  ( $k = 0, \dots, n$ ) are complex expansion coefficients. In general, the maximally entangled symmetric state of  $n$  qubits is a superposition of Dicke states. Note that  $\mathbb{C}^N$  is the symmetric subspace we obtain by taking the tensor product of  $\mathbb{C}^2$  with itself  $N$  times.

As stated in Section 2.2 it is possible to uniquely represent a pure state of spin- $j$  by  $2j$  undistinguishable points on the sphere via the stellar representation, here known as the Majorana representation. This representation is useful for obtaining an expression for the geometric measure of entanglement for any symmetric  $n$ -qubit state  $|\psi\rangle_S$ .

The Majorana representation allows us to compose any symmetric state  $|\psi\rangle_S$  of  $n$  qubits from a sum over all permutations  $P : S_n \rightarrow S_n$  of  $n$  undistinguishable qubits  $\{|\phi_1\rangle, \dots, |\phi_n\rangle\}$ :

$$|\psi\rangle_S = \frac{1}{\sqrt{K}} \sum_{\text{perm}} |\phi_{P(1)}\rangle \cdots |\phi_{P(n)}\rangle, \quad (5.3)$$

with

$$|\phi_i\rangle = \cos \frac{\theta_i}{2} |0\rangle + e^{i\varphi_i} \sin \frac{\theta_i}{2} |1\rangle \quad (5.4)$$

and where the normalization factor  $K$  depends on the given state.

(5.4) allows the visualization of the qubit state  $|\psi\rangle_S$  by  $n$  unordered points on a sphere at the position  $(\theta_i, \phi_i)$ . Any arrangement of  $n$  points on the unit sphere thus defines a symmetric state. From now on, we will call these points the Majorana points (MP).

Point distributions are invariant under local unitary maps. This means that the product of local unitary maps on a symmetric state,  $U \otimes U \otimes \dots \otimes U |\psi\rangle_S$ , is nothing more than a rotation of the sphere upon which we have placed our points, since each point gets rotated by the same  $U$ . As a result the entanglement remains unchanged under rotation.

## 5.1 Geometric Measure of Entanglement

In this section we introduce a way of quantifying the amount of entanglement of a state, which is given by the geometric measure of entanglement. This is a distance-like entanglement measure in the sense that it assesses the entanglement in terms of the remoteness from the set of separable states. Following Ref. [38] we derive and simplify the expression for the maximized entanglement measure.

A general quantum state of a finite-dimensional system can be written as  $|\psi\rangle = \sum_i a_i |i\rangle$  with complex coefficients  $a_i$  and an orthonormal basis  $\{|i\rangle\}$ . The state  $|\psi\rangle$  is called positive if the  $a_i$  are all positive. Every positive state  $|\psi\rangle$  has at least one positive closest product state  $|\Lambda_\psi\rangle = \otimes_j |\sigma_j\rangle$ , where  $|\sigma_j\rangle = \sum_{i_j} b_{i_j}^j |i_j\rangle$  (with  $b_{i_j}^j \in \mathbb{C}$ ) is the state of subsystem  $j$ .



The geometric measure of entanglement is defined as the maximal overlap of a normalized pure state  $|\psi\rangle$  with all normalized pure product states:

$$E_G(|\psi\rangle) = \min_{|\lambda\rangle \in H_{\text{SEF}}} \log_2 \left( \frac{1}{|\langle \lambda | \psi \rangle|^2} \right), \quad (5.5)$$

where the minimum is taken over all separable pure states. A finite-dimensional Hilbert space always contains at least one state  $|\Psi\rangle$  with maximal entanglement, and each such state can have more than one closest product state. Let us denote a product state closest to  $|\psi\rangle$  by  $|\Lambda_\psi\rangle$ . Then the task of maximizing the entanglement measure can be written as a max-min problem

$$E_G^{\text{max}} = \max_{|\psi\rangle \in H} \min_{|\lambda\rangle \in H_{\text{SEF}}} \log_2 \left( \frac{1}{|\langle \lambda | \psi \rangle|^2} \right) \quad (5.6)$$

$$= \log_2 \left( \frac{1}{|\langle \Lambda_\Psi | \Psi \rangle|^2} \right). \quad (5.7)$$

The problem now consists of finding the closest product state to a given quantum state. This is simplified by considering permutation-symmetric states, which are states that are invariant under any permutation of their subsystems, i.e.  $P|\psi\rangle = |\psi\rangle$  for all  $P \in S_n$ .

### Closest Product Point

For  $n \geq 3$  qubits, every closest product state  $|\Lambda\rangle_S$  of a symmetric state  $|\psi\rangle_S$  is symmetric itself and can therefore be written as  $|\Lambda\rangle_S = |\sigma\rangle^{\otimes n}$ , where  $|\sigma\rangle$  is a single qubit state. The closest product states of a given symmetric state can be visualized by Bloch vectors of  $|\sigma\rangle$ . We will refer to  $|\sigma\rangle$  as a closest product point (CPP).

For symmetric product states  $|\lambda\rangle = |\sigma\rangle^{\otimes n}$  the scalar product in the definition of the geometric measure can be expressed in terms of the MPs and a CPP:

$$|\langle \lambda | \psi \rangle_S| = \frac{n!}{\sqrt{K}} \prod_{i=1}^n |\langle \sigma | \phi_i \rangle|. \quad (5.8)$$

The factors  $\langle \sigma | \phi_i \rangle$  are the angles between the corresponding Bloch vectors on the Majorana sphere. As stated before, the problem of finding the maximal entanglement measure can be simplified to finding the CCP of a given quantum state. Now, to determine the CPP of a given symmetric state, we have to maximize the absolute value of a product of scalar products, giving us a geometrical optimization problem. We can simplify the problem further, since the maximization is only required on the restricted set of symmetric separable states  $|\phi_1\rangle, \dots, |\phi_n\rangle$ . Then by inserting (5.8) into (5.7) we obtain

$$E_G(|\psi_S\rangle) = 1 - \frac{n!}{\sqrt{K}} \max_{|\phi\rangle} \prod |\langle \sigma | \phi_i \rangle|^2. \quad (5.9)$$

Hence, the optimization problem of finding the entanglement measure has the geometric interpretation of maximizing the product of angles  $|\langle \sigma | \phi_i \rangle|^2$ .

## 5.2 Highest Geometric Entanglement Configurations

The problem of finding the maximally entangled symmetric state can be understood as an optimization problem on the sphere, prompting the question whether the known solutions to spherical point distribution problems can help us find the solutions of the Majorana problem. The geometric phrasing of the problem allows us to use geometric properties, for example symmetry of the MP distribution, to calculate entanglement and to search for the most entangled states in this class. In a sense, we can say that the most entangled states will be those that spread out the points the most.

In this section we present maximal entanglement configurations together with those arrangements of MPs that correspond to the maximal Wehrl Entropy for 2-9 points (see Tables 4.1, 4.2). The arrangements corresponding to maximal Wehrl entropy are expected to provide high entanglement configurations in view of their anti coherent spin states, even though they do not necessarily provide the most geometrically entangled symmetric states.

We now present the value of the maximal geometric measure of entanglement  $E_G(|\psi\rangle)$  for 2-9 points and compare the corresponding configurations to the arrangements that correspond to a maximized Wehrl entropy. The Majorana representations of the most entangled symmetric states are presented in Fig. 5.1 and Fig. 5.2, where the maximal entanglement arrangements are shown for 2-9 points together with the arrangements that correspond to a maximized Wehrl entropy. Note that these states are characterized by  $n$  distinct points on the Bloch sphere with a large spread.

- $n = 2$ : For two qubits the maximally entangled state is identified as the Bell state  $|\psi_2\rangle = (|00\rangle + |11\rangle)/\sqrt{2}$  with  $E_G(|\psi^+\rangle) = 1$ . The corresponding configuration consists of two points diametrically opposite to each other on the sphere. Thus the Majorana representation of the most geometrically entangled symmetric states coincides with the configuration that yields maximal Wehrl entropy.
- $n = 3$ : For three qubits the maximally entangled state is identified as  $|\psi_3\rangle = |S_{3,1}\rangle$  with  $E_G(|S_{3,1}\rangle) \approx 1.17$ . In this case the corresponding configuration does not coincide with the configuration that yields maximal Wehrl entropy, which is given by three points forming an equilateral triangle on a large circle.
- $n = 4$ : For four qubits the maximally entangled state is given by  $|\Psi_4\rangle = \frac{1}{\sqrt{3}}|S_0\rangle + \sqrt{\frac{2}{3}}|S_3\rangle$  with  $E_G(|\Psi_4\rangle) \approx 1.58$ . The corresponding configuration consists a platonic solid, namely the tetrahedron. Thus the Majorana representation of the most geometrically entangled symmetric states coincides with the configuration that yields maximal Wehrl entropy.
- $n = 5$ : For five qubits the maximally entangled state is given by  $|\Psi_5\rangle \approx 0.547|S_1\rangle + 0.837|S_4\rangle$  with  $E_G(|\Psi_5\rangle) \approx 1.74$ . In this case the corresponding

configuration in the form of a square pyramid does not coincide with the configuration that yields maximal Wehrl entropy, which is given by three equidistant points on the equator together with two points at the poles, placed diametrically opposite each other.

- $n = 6$ : For six qubits the maximally entangled state is given by  $|\Psi_6\rangle = \frac{1}{\sqrt{2}}(|S_1\rangle + |S_5\rangle)$  with  $E_G(|\Psi_6\rangle) \approx 2.17$ . The corresponding configuration consists of a regular polyhedra, namely the octahedron. Thus the Majorana representation of the most geometrically entangled symmetric states coincides with the configuration that yields maximal Wehrl entropy.
- $n = 7$ : For seven qubits the maximally entangled state is given by  $|\Psi_7\rangle = \frac{1}{\sqrt{2}}(|S_1\rangle + |S_6\rangle)$  with  $E_G(|\Psi_7\rangle) \approx 2.299$ . The corresponding configuration consists of a pentagonal dipyrmaid, where five points lie on an equatorial pentagon and the other two on the poles. Thus the Majorana representation of the most geometrically entangled symmetric states coincides with the configuration that yields maximal Wehrl entropy.
- $n = 8$ : For eight qubits the maximally entangled state is given by  $|\Psi_8\rangle \approx 0.672|S_1\rangle + 0.741|S_6\rangle$  with  $E_G(|\Psi_8\rangle) \approx 2.299$ . The corresponding configuration is in the form of three equidistant points on the equator together with two points at the North pole and one at the South pole. This does not coincide with the configuration that yields maximal Wehrl entropy, which is a cubic antiprism. The state vector for the cubic antiprism is given by [44]  $|\psi_8^g\rangle = (|S_0\rangle + A|S_4\rangle - |S_8\rangle)/(\sqrt{2 + A^2})$  with  $E_G(|\psi_8^g\rangle) \approx 2.23$ . The real parameter  $A = 1.64451$  depends on the latitude of the MP rings.
- $n = 9$ : For nine qubits the maximally entangled state is given by  $|\Psi_9\rangle = \frac{1}{\sqrt{2}}(|S_2\rangle + |S_7\rangle)$  with  $E_G(|\Psi_9\rangle) \approx 2.554$ . The corresponding configuration is a pentagonal dipyrmaid state. This does not coincide with the configuration that yields maximal Wehrl entropy, which is a triaugmented triangular prism state consisting of three equilateral triangles are positioned parallel but asymmetric to each other. The state vector for the triaugmented triangular prism state is given by [44]  $|\psi_9\rangle = (|S_0\rangle - A(|S_3\rangle + |S_6\rangle) + |S_9\rangle)/(\sqrt{2 + 2A^2})$  with  $E_G(|\psi_9\rangle) \approx 2.532$  and  $A \approx -1.37568$ .

We have thereby presented the configurations that correspond to the maximally entangled states. We have compared the geometric measure of entanglement for these arrangements, to the geometric measure of entanglement given by configurations corresponding to maximal Wehrl entropy. Our results are presented in Fig. 5.1 and Fig. 5.2. We note that although the non-coherent states correspond to high values of geometric entanglement, they do not necessarily correspond to the most entangled states.

Figure 5.1: The geometric measure of entanglement (GMET) for configurations corresponding to the most entangled symmetric states and configurations corresponding to maximal Wehrl entropy for  $n = 2-5$  points on a sphere. Here  $n$  is the number of points for dimension  $N = n + 1$  and  $GMET$  is the geometric measure of entanglement.

















	Maximal $S_W$	Maximal GMET
$n = 2$		
State Vector	$ \psi^+\rangle = \frac{1}{\sqrt{2}}( 01\rangle +  10\rangle)$	$ \psi^+\rangle = \frac{1}{\sqrt{2}}( 01\rangle +  10\rangle) =  S_1\rangle$
GMET	$E_G( \psi^+\rangle) = 1$	$E_G( \psi^+\rangle) = 1$
$n = 3$		
State Vector	$ \psi_3\rangle = \frac{1}{\sqrt{2}}( 000\rangle +  111\rangle)$	$ S_{3,1}\rangle = \frac{1}{\sqrt{3}} \sum_{\text{perm}}  001\rangle$
GMET	$E_G( \psi_3\rangle) = 1$	$E_G( S_{3,1}\rangle) \approx 1.17$
$n = 4$		
State Vector	$ \psi_4\rangle = \frac{1}{\sqrt{3}} S_0\rangle + \sqrt{\frac{2}{3}} S_3\rangle$	$ \psi_4\rangle = \frac{1}{\sqrt{3}} S_0\rangle + \sqrt{\frac{2}{3}} S_3\rangle$
GMET	$E_G( \psi_4\rangle) \approx 1.58$	$E_G( \psi_4\rangle) \approx 1.58$
$n = 5$		
State Vector	$ \psi_5\rangle = \frac{1}{\sqrt{2}}( S_1\rangle +  S_4\rangle)$	$ \psi_5\rangle \approx 0.547 S_1\rangle + 0.837 S_4\rangle$
GMET	$E_G( \psi_5\rangle) \approx 1.68$	$E_G( \psi_5\rangle) \approx 1.74$

Figure 5.2: The geometric measure of entanglement (GMET) for configurations corresponding to the most entangled symmetric states and configurations corresponding to maximal Wehrl entropy for  $n = 6-9$  points on a sphere. Here  $n$  is the number of points for dimension  $N = n + 1$  and  $GMET$  is the geometric measure of entanglement.

	Maximal $S_W$	Maximal GMET
$n = 6$		
State Vector	$ \psi_6\rangle = \frac{1}{\sqrt{2}} ( S_1\rangle +  S_5\rangle)$	$ \psi_6\rangle = \frac{1}{\sqrt{2}} ( S_1\rangle +  S_5\rangle)$
GMET	$E_G( \psi_6\rangle) \approx 2.17$	$E_G( \psi_6\rangle) \approx 2.17$
$n = 7$		
State Vector	$ \psi_7\rangle = \frac{1}{\sqrt{2}} ( S_1\rangle +  S_6\rangle)$	$ \psi_7\rangle = \frac{1}{\sqrt{2}} ( S_1\rangle +  S_6\rangle)$
GMET	$E_G( \psi_7\rangle) \approx 2.299$	$E_G( \psi_7\rangle) \approx 2.299$
$n = 8$		
State Vector	$ \psi_8^a\rangle = \frac{ S_0\rangle + A( S_4\rangle -  S_8\rangle)}{\sqrt{2+A^2}}$	$ \psi_8\rangle \approx 0.672 S_1\rangle + 0.741 S_6\rangle$
GMET	$E_G( \psi_8^a\rangle) \approx 2.23$	$E_G( \psi_8\rangle) \approx 2.45$
$n = 9$		
State Vector	$ \psi_9\rangle = \frac{ S_0\rangle - A( S_3\rangle +  S_6\rangle) +  S_9\rangle}{\sqrt{2+2A^2}}$	$ \psi_9\rangle = \frac{1}{\sqrt{2}} ( S_2\rangle +  S_7\rangle)$
GMET	$E_G( \psi_9\rangle) \approx 2.532$	$E_G( \psi_9\rangle) \approx 2.554$



## Chapter 6

# Summary and Conclusions

In this chapter we summarize the investigations described in this thesis. We began our investigation by introducing the Bloch sphere and establishing a one-to-one correspondence between the Bloch sphere and the extended complex plane by means of stereographic projection. Under the assumption that the Hilbert space is finite-dimensional, the state space may be regarded as a complex projective space. This could be visualized in real terms by means of the stellar representation, so that vectors in the complex projective space are represented by unordered sets of points on a Bloch sphere. We continued by considering coherent states, with an emphasis on Bloch coherent states, which are the most classical quantum states. We noted that the Bloch coherent states are the only states for which all points on the sphere coincide in the stellar representation.

Following Ref. [1] we introduced the Husimi function (4.6), and presented the Wehrl entropy in terms of Bloch coherent states

$$S_W(|\psi\rangle\langle\psi|) \equiv -\frac{n+1}{4\pi} \int_{\Omega} d\Omega Q_{\psi}(z) \ln Q_{\psi}(z), \quad (6.1)$$

where  $Q_{\psi}(z)$  is the Husimi function. We gave a short explanation of the significance of the Wehrl entropy as a measure of how classical a system is, and described the Lieb conjecture, which states that the Wehrl entropy attains its minimum for Bloch coherent states. Using the stellar representation and methods described in Ref. [16,17], we calculated the entropy integral (6.1).

We continued by considering the Wehrl entropy for the most non-coherent states, which we define as the states that maximize the Wehrl entropy. More specifically, we considered spherical arrangements of 2-9 points in order to identify configurations for which local maxima of the Wehrl entropy occur. To this end we compared configurations that solve the Thomson problem [22], the Toth problem [23] and the QQ problem [24]. We found that the configurations that solve the Thomson problem, the Toth problem and the QQ problem also yield local maxima of the Wehrl entropy for up to seven dimensions. In higher dimensions the arrangements

that solve the Thomson problem, the Toth problem and the QQ problem no longer maximize the Wehrl entropy, but by varying parameters in the solutions for these problems we were able to find local maxima of the Wehrl entropy. We conjectured that the local maxima also are global maxima.

Following Ref. [25] we gave a geometric illustration of how quantum channels for coherent states majorize all other quantum channels. We considered the spectra of the Wehrl entropy and the von Neumann entropy, and showed that maximal Wehrl entropy and von Neumann entropy occur for the most non-coherent states, and that minimal Wehrl entropy and von Neumann entropy occur for the coherent states.

Furthermore, we presented a geometrical interpretation of the entanglement of permutation symmetric states in the form of the Majorana representation according to Ref. [38]. We calculated the maximally entangled symmetric states of 2-9 qubits and their amount of geometric entanglement. Finally, we discussed how these maximally entangled symmetric states are related to the states corresponding to maximal Wehrl entropy. We conclude that although the most non-coherent states yield high values of geometric entanglement, they do not necessarily correspond to the most entangled states.



# Bibliography

- [1] I Bengtsson, K Życzkowski, *Geometry of Quantum States: An Introduction to Quantum Entanglement*, Cambridge University Press (2006).
- [2] E Majorana, *Atomi orientati in campo magnetico variabile*, Nuovo Cimento **9**, 43 (1932).
- [3] R Penrose, *Shadows of the mind: A search for the missing science of consciousness*, Vintage (2005).
- [4] H Bacry, *Orbits of the rotation group on spin states*, J. Math. Phys. **15**, 10 (1974).
- [5] Q Niu, *Viewpoint: A Quantum Constellation*, Physics **5**, 65 (2012).
- [6] J P Gazeau, *Coherent States in Quantum Physics*, WILEY-VCH Verlag (2009).
- [7] J M Radcliffe, *Some properties of coherent spin states*, J. Phys. A: Gen. Phys. **4**, 313 (1971).
- [8] J P Antoine, *Contemporary Problems in Mathematical Physics*, World Scientific (2000).
- [9] R W Henry, S C Glotzer, *A squeezed-state primer*, Am. J. Phys. **56**, 4 (1988).
- [10] C Gross, *Spin Squeezing and Non-linear Atom Interferometry with Bose-Einstein Condensates*, Springer-Verlag (2012).
- [11] A Miranowicz, H Matsueda, M R B Wahiddin, *Classical information entropy and phase distributions of optical fields*, J. Phys. A: Math. Gen. **33**, 5159 (2000).
- [12] A Vourdas, *Analytic representations in quantum mechanics*, J. Phys. A: Math. Gen. **39**, R65 (2006).
- [13] R Delbourgo, *Minimal uncertainty states for the rotation group and allied groups*, J. Phys. A: **10**, L233 (1977).

- [14] J D Bukweli-Kyemba, M N Hounkonnou, *Quantum deformed algebras: coherent states and special functions*, arXiv:1301.0116v1 [math-ph] (2013).
- [15] E H Lieb, *Proof of an entropy conjecture of Wehrl*, Commun. Math. Phys. **62**, 35 (1978).
- [16] C T Lee, *Wehrl's entropy of spin states and Lieb's conjecture*, J. Phys. A: Math. Gen. **21**, 3749 (1988).
- [17] P Schupp, *On Lieb's conjecture for the Wehrl entropy of Bloch coherent states*, Commun. Math. Phys. **207**, 481 (1999).
- [18] R Clausius, *Abhandlungen uber die mechanische warmetheorie*, Braunschweig (1864).
- [19] A Wehrl, *General properties of entropy*, Rev. Mod. Phys., **50**, 221 (1978).
- [20] A Wehrl, *On the relation between classical and quantum mechanical entropies*, Rep. Math. Phys., **16**, 353 (1979).
- [21] G B Bodmann, *A lower bound for the Wehrl entropy of quantum spin with sharp high-spin asymptotics*, Commun. Math. Phys. **250**, 287 (2004).
- [22] G B Thomson, *On the structure of the atom: an investigation of the stability and periods of oscillation of a number of corpuscles arranged at equal intervals around the circumference of a circle; with application of the results to the theory of atomic structure*, Phil. Mag. **39**, 237 (1904).
- [23] L Fejes-Toth, *On the densest packing of spherical caps*, Am. Math. Monthly **56**, 330 (1949).
- [24] O Giraud, P A Braun, D Braun, *Quantifying Quantumness and the Quest for Queens of Quantum*, New J. Phys. **12**, 063005 (2010).
- [25] E H Lieb, J P Solovej, *Proof of an entropy conjecture for Bloch coherent spin states and its generalizations*, arXiv:1208.3632v2 [math-ph] (2012).
- [26] M Atiyah, P Sutcliffe, *Polyhedra in physics, chemistry and geometry*, Milan J. Math. **71**, 33 (2003).
- [27] C Anastopoulos, *Information measures and classicality in quantum mechanics*, Phys. Rev. D **59**, 045001 (1999).
- [28] D Petz, *Entropy, von Neumann and the von Neumann entropy*, arXiv:0102013v1 [math-ph] (2001).
- [29] H Y Fan, Q Guo, *Husimi operator and Husimi function for describing electron's probability distribution in uniform magnetic field derived by virtue of the entangled state representation*, arXiv:0611206v1 [quant-ph] (2006).

- [30] M M Wilde, *From Classical to Quantum Shannon Theory*, arXiv:1106.1445v5 [quant-ph] (2013).
- [31] J R Edmundson, *The distribution of point charges on the surface of a sphere*, Acta Cryst. A **48**, 60 (1992).
- [32] B Bagchi, *How to stay away from each other in a spherical universe*, Resonance **2**, 10 (1997).
- [33] T Erbert, G M Hockney, *Equilibrium configurations of  $N$  equal charges on a sphere*, J. Phys. A: Math. Gen. **21**, L1369 (1991).
- [34] L L Whyte, *Unique Arrangements of Points on a Sphere*, Amer. Math. Monthly **59**, 9 (1952).
- [35] J Schwinger, *The Geometry of Quantum States*, Proc. Natl. Acad. Sci. USA **46**, 2 (1960).
- [36] N Ashby, W E Brittin, *Thomson's problem*, Am. J. Phys. **54**, 9 (1986).
- [37] A A Berezin, *Simple electrostatic model of the structural phase transition*, Am. J. Phys. **54**, 403 (1986).
- [38] M Aulbach, D Markham, M Murao, *The maximally entangled symmetric state in terms of the geometric measure*, New J. Phys. **12**, 073025 (2010).
- [39] R Hübener, M Kleinmann, T C Wei, C González-Guillén, Otfried Gühne, *The geometric measure of entanglement for symmetric states*, Phys. Rev. A **80**, 032324 (2009).
- [40] J Martin, O Giraud, P A Braun, D Braun, T Bastin, *Multiqubit symmetric states with high geometric entanglement*, Phys. Rev. A **81**, 062347 (2010).
- [41] D J H Markham, *Entanglement and symmetry in permutation symmetric states*, Phys. Rev. A **83**, 042332 (2011).
- [42] M Aulbach, D Markham, M Murao, *Geometric Entanglement of Symmetric States and the Majorana Representation*, arXiv:1010.4777v1 [quant-ph] (2010).
- [43] R B Lockhart, M J Steiner, K Gerlach, *Geometry and product states*, Quantum Info. and Comp. **2**, 333 (2002).
- [44] M Aulbach, *Classification of Entanglement in Symmetric States*, PhD thesis, University of Leeds, (2011).



## Appendix A

### SU(2)

The generators of  $SU(2)$  in the fundamental representation are the Pauli matrices  $\vec{\sigma} = \{\sigma_x, \sigma_y, \sigma_z\}$ ,

$$\sigma_x = \begin{bmatrix} 0 & 1 \\ 1 & 0 \end{bmatrix}, \quad \sigma_y = \begin{bmatrix} 0 & -i \\ i & 0 \end{bmatrix}, \quad \sigma_z = \begin{bmatrix} 1 & 0 \\ 0 & -1 \end{bmatrix}. \quad (\text{A.1})$$

There is one unitary representation of  $SU(2)$  in every dimension  $N = n+1 = 2j+1$ , with generators

$$J_x = \frac{1}{2} \begin{bmatrix} 0 & \sqrt{n} & 0 & \dots \\ \sqrt{n} & 0 & \sqrt{2(n-1)} & \dots \\ 0 & \sqrt{2(n-1)} & 0 & \dots \\ \vdots & \vdots & \vdots & \ddots \end{bmatrix} \quad (\text{A.2})$$

$$J_y = \frac{i}{2} \begin{bmatrix} 0 & -\sqrt{n} & 0 & \dots \\ \sqrt{n} & 0 & -\sqrt{2(n-1)} & \dots \\ 0 & \sqrt{2(n-1)} & 0 & \dots \\ \vdots & \vdots & \vdots & \ddots \end{bmatrix} \quad (\text{A.3})$$

$$\text{and } J_z = \begin{bmatrix} n & 0 & 0 & \dots \\ 0 & n-2 & 0 & \dots \\ 0 & 0 & n-4 & \dots \\ \vdots & \vdots & \vdots & \ddots \end{bmatrix}. \quad (\text{A.4})$$

These generators of  $SU(2)$  correspond to rotation of the sphere around the three orthogonal axes  $x$ ,  $y$  and  $z$ .